

Contents lists available at [ScienceDirect](https://www.sciencedirect.com)

# Mechanical Systems and Signal Processing

journal homepage: [www.elsevier.com/locate/ymssp](http://www.elsevier.com/locate/ymssp)

## Vibration fatigue by spectral methods—A review with open-source support

Aleš Zorman, Janko Slavič\*, Miha Boltežar

University of Ljubljana, Faculty of Mechanical Engineering, Aškerčeva 6, 1000, Ljubljana, Slovenia

### ARTICLE INFO

Communicated by J. Antoni

Dataset link: <https://github.com/ladisk/FLife>

#### Keywords:

Vibration fatigue  
Spectral methods  
Random process  
Broadband  
Open source

### ABSTRACT

Vibration fatigue by spectral methods relates the theory of structural dynamics to high-cycle vibration fatigue. An ideal spectral method should perform well and consistently, regardless of the response spectrum and the material being analyzed. The primary aim of this review is to develop a common theoretical and open-source-code framework for a side-by-side comparison of more than 20 spectral methods, which will help a future spectral-domain vibration-fatigue research. The reviewed spectral methods are structured in terms of the damage-estimation concept: narrowband approximation, narrowband correction factor (Wirsching–Light, Ortiz–Chen,  $\alpha_{0.75}$ , Tovo–Benasciutti (two versions)), rainflow probability-density-function approximation (Dirlik, Zhao–Baker, Park, Jun–Park) and combined fatigue damage, where the damage is combined according to the cycle types (Jiao–Moan, Sakai–Okamura, Fu–Cebon, modified Fu–Cebon, Low’s bimodal, Low 2014, Gao–Moan) and the narrowband damage combination criterion (Lotsberg, Huang–Moan, single moment, bands method). All the reviewed methods are implemented in the supporting open-source Python package FLife, with the comparison being fully reproducible using the package documentation. The accuracy of the spectral methods is investigated in terms of a time-domain rainflow analysis, where three different materials are considered: steel, aluminium and spring steel. The comparison is based on typical PSD defined signals, with the focus on: spectral width, background noise, close modes, number of modes and typical vibration profiles used in accelerated automotive tests. In addition, a bimodal spectrum is formulated to examine a specific group of spectral methods that are developed for bimodal random processes. This research shows that other methods, besides the well-established ones, such as the Dirlik and Tovo–Benasciutti methods, should be considered when the fatigue load is broadband: Ortiz–Chen,  $\alpha_{0.75}$ , Park, Jun–Park and Huang–Moan methods. Furthermore, as the fatigue analysis of bimodal random processes has become well established, the applicability of bimodal methods is inspected. Among the reviewed spectral methods, Low’s bimodal and Low 2014 method show exceptional accuracy that can be attained using the bimodal formulation.

### 1. Introduction

Vibration fatigue using spectral methods relates the theory of structural dynamics to damage estimation in the frequency domain [1]. Random fatigue loads (e.g., due to irregularities in the road or due to waves at sea) can be viewed as the realization of a stationary Gaussian process, represented by the power spectral density (PSD) [2]. The classical approach to fatigue loading is in the time domain, where the fatigue estimation typically starts by identifying the damage cycles with the rainflow-counting

\* Corresponding author.

E-mail address: [janko.slavic@fs.uni-lj.si](mailto:janko.slavic@fs.uni-lj.si) (J. Slavič).

<https://doi.org/10.1016/j.ymssp.2023.110149>

Received 12 July 2022; Received in revised form 9 December 2022; Accepted 21 January 2023

Available online 30 January 2023

0888-3270/© 2023 The Author(s).

Published by Elsevier Ltd.

This is an open access article under the CC BY license

(<http://creativecommons.org/licenses/by/4.0/>).

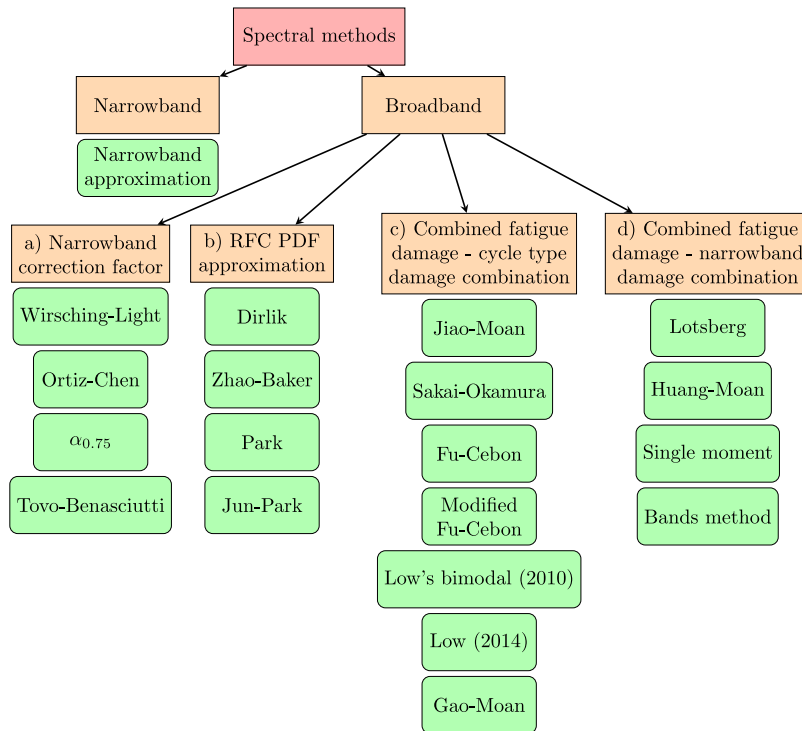


Fig. 1. Reviewed spectral methods.

algorithm [3–5]. Once these cycles are identified, the fatigue damage is aggregated according to the hypothesis of linear damage accumulation, which was independently described by Palmgren [6] and Miner [7]. Since damage accumulation model greatly affects the fatigue-life estimate, many other deterministic models, such as bilinear [8,9] and trilinear rules or sigmoidal curves [10,11] are often applied to accommodate for material characteristics. A comparative review of time- and frequency-domain methods for fatigue damage assessment is given by Muñiz-Calvente et al. [12]. However, the combination of rainflow counting and the Palmgren–Miner rule has been tried and tested and is generally accepted as a reference to check the accuracy of frequency-domain spectral methods [13–15].

Frequency-domain vibration-fatigue by spectral methods extends the theory of structural dynamics [1] and not only significantly speeds-up the numerical evaluation of large models (e.g., due to modal decomposition [16,17]), but also offers to relate the dynamic loads to the well-established theory of random processes [2,5]. In the structural dynamics theory, the excitation is related to the response via the frequency response functions [18]. In recent years the excitation was significantly researched for multi-axis excitation [19,20], while the excitation and response have been significantly researched for non-Gaussianity [21] or/and non-stationarity [22,23]. At the response, a special attention is required for multiaxial loads [24,25]; for multiaxial loads the state of the art approach is to use an uniaxial equivalent approach [26]. Since numerous engineering applications are neither Gaussian nor stationary, a lot of effort was put into applying the spectral methods to non-Gaussian [27–29], non-stationary [30–32] and sine-on-random environment [33–35]. This research is focused on the uni-axial fatigue damage in the frequency-domain, where a zero-mean stationary Gaussian random process is assumed.

However, only for the narrowband Gaussian process can the fatigue damage be theoretically estimated with the Rayleigh stress range distribution [36,37]. For a general broadband process, the correlation between the distribution of rainflow cycles and the spectral density is so complex that the theoretical framework behind the frequency-domain fatigue analysis has no theoretically exact solution [38].

If the narrowband fatigue damage model were to be applied to broadband processes, conservative predictions of the damage with respect to the rainflow-counting scheme would be obtained [39]. Consequently, for broadband Gaussian random processes, numerous spectral methods have been researched (theoretically and empirically). In this review the broadband spectral methods are structured according to the fatigue-damage estimation concept, as shown in Fig. 1: (a) narrowband correction factor, (b) rainflow probability density function (PDF) approximation, (c) combined fatigue damage - cycle type damage combination and (d) combined fatigue damage - narrowband damage combination.

**Narrowband correction factor.** A correction factor for the narrowband fatigue-damage model expands its applicability to broadband processes. Several spectral methods have been devised according to this concept (Fig. 1, (a)). Wirsching and Light [40] empirically determined a correction factor based on the spectral width and the material used. Ortiz and Chen [41] introduced a generalized

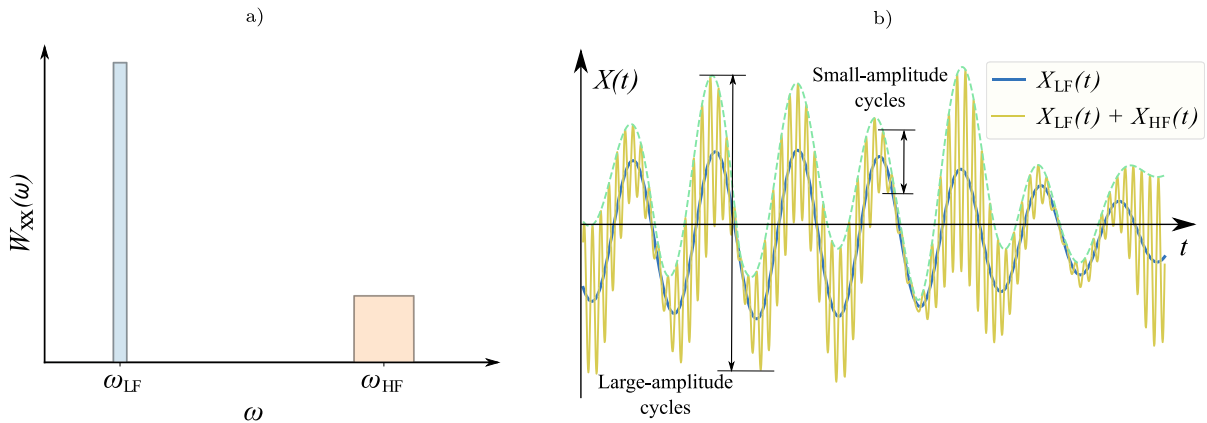


Fig. 2. Bimodal random process; (a) PSD, (b) time history illustrating the small- and large-amplitude cycles.

spectral bandwidth parameter, which also depends on the material's S-N curve. A simple yet effective method was proposed by Tovo and Benasciutti [42], which depends only on the  $\alpha_{0.75}$  bandwidth parameter. Another spectral method by Tovo and Benasciutti [14,43] is based on a combination of the upper and lower damage intensity limits, with two correction factors defined. This method also supports the rainflow PDF approximation.

*Rainflow PDF approximation.* Among the spectral methods that approximate the rainflow stress cycle PDF on the basis of PSD (Fig. 1, (b)) and then continue towards damage identification, the pioneering work was performed by Dirlik [44]. Dirlik modeled the rainflow PDF by combining one exponential and two Rayleigh probability densities. Several other methods have been proposed. The Zhao and Baker [45] method gives the rainflow PDF in the form of a linear combination of the Weibull and Rayleigh PDF. Park et al. [46] presented a method where they approximate the rainflow PDF with a combination of Rayleigh, a standard Rayleigh and a half-Gaussian distribution. Similarly, the spectral method of Jun and Park [47] approximates the rainflow PDF with a Rayleigh, a standard Rayleigh, a half-Gaussian and an additional exponential distribution.

*Combined fatigue damage - cycle type damage combination.* Special cases of broadband random processes are the multimodal processes, whose spectral density is formed by the superposition of two or more well separated narrowband contributions. By analyzing these processes in the time domain, clearly distinguishable classes of stress cycles can be observed, e.g., for bimodal processes a small-amplitude and large-amplitude, as shown in Fig. 2(b). Spectral methods in the cycle type damage combination group (Fig. 1, (c)) estimate damage for each cycle type independently. By summing the damage contributions of all cycle categories the combined fatigue damage is obtained. A pioneering work by Jiao and Moan [48] on bimodal fatigue analysis considers small-amplitude cycles being attributed entirely to the high-frequency component, whereas large-amplitude cycles are associated with both low- and high-frequency components. In the last period we have seen generalizations to multi-modal loads. Here, the following bimodal spectral methods will be reviewed: Jiao-Moan [48], Sakai-Okamura [49], Fu-Cebon [50], modified Fu-Cebon [51], Low's bimodal [52] and Low-2014 [53]. Additionally, the trimodal method by Gao and Moan [54], which can be generalized for a general broadband random process, will also be reviewed.

*Combined fatigue damage - narrowband damage combination.* Provided that the broadband stress spectrum is decomposed into a set of narrowband spectral contributions, fatigue damage can be calculated for each infinitesimal sub-band using the narrowband approximation. Such approach (Fig. 1, (d)) is convenient for practical applications because the combined fatigue damage is expressed as an explicit form of individual narrowband damage contributions. As the relation of the stress and fatigue damage is nonlinear, the combined fatigue damage is not simply the sum of individual damages and a suitable combination rule should be employed [55,56]. This research will review the following spectral methods from the narrowband damage-combination category: Lotsberg [57], Huang-Moan [58], single-moment method [59,60] and bands method [61]. Lotsberg and Huang-Moan spectral methods were devised for bimodal random process. As for a general broadband random process, the single-moment method by Lutes and Larsen [59,60] is essentially a spectral decomposition method, where the quadratic amplitude sum of the "Projection-by-Projection" (PbP) multiaxial vibration fatigue criterion [62] is employed as a damage-combination rule. In contrast to the empirical single-moment method, Braccisi et al. [61] presented the bands method, which was derived theoretically, although the damage-combination rule used is equivalent to a quadratic amplitude sum of the PbP criterion [63]. Another reviewed fatigue-damage method that employs the PbP criterion was proposed by the Han and Ma [64], with applicability to bimodal random processes.

Since the spectral methods were developed with respect to particular spectra, they should be assessed as to whether they give reliable fatigue-damage predictions for the various response spectra to which they might be applied. Many comparison studies of spectral methods are available in literature. Benasciutti and Tovo [65] compared several spectral methods for the fatigue analysis of a broadband Gaussian random process, i.e., the narrowband formulation [36], Wirsching-Light [40], Dirlik [44], Zhao-Baker [45], Tovo-Benasciutti [14,43] and  $\alpha_{0.75}$  [42], and concluded that the Tovo-Benasciutti method matches the accuracy of the Dirlik method

in terms of numerically simulated power spectral densities. According to Mršnik et al. [15], who in addition to methods compared by Benasciutti and Tovo also investigated the accuracy of the Petrucci–Zuccarello [66] and Gao–Moan [54] methods, the Tovo–Benasciutti method appears to be the best, followed by the Zhao–Baker and Dirlik methods. Based on the comprehensive review by Mršnik et al., in 2015 Larsen and Irvine [67] compared the narrowband formulation [36], Wirsching–Light [40], Ortiz–Chen [41], Tovo–Benasciutti [14,43],  $\alpha_{0.75}$  [42], Dirlik [44] and the single-moment [59,60] method. For the purposes of comparison, Larsen and Irvine studied the above methods with respect to the same spectra types as those used by Mršnik et al. [15] and concluded that for a large S-N slope parameter [68] ( $k=12$ ) all the spectral methods exhibit substantial errors, but the  $\alpha_{0.75}$  and single-moment methods can still be acceptable [67]. Similar conclusions were drawn by Quijley et al. [69] in 2016, where in order of preference, the  $\alpha_{0.75}$ , Ortiz–Chen, Dirlik, Tovo–Benasciutti and single-moment methods were advocated. Spectral methods for a fatigue-damage estimation in bimodal random processes were compared by Benasciutti and Tovo [51] in 2005; single-moment [59,60], Jiao–Moan [48], Sakai–Okamura [49], Fu–Cebon [50], modified Fu–Cebon [51] and Tovo–Benasciutti [14,43] method were reviewed. Among these methods, the single-moment, Tovo–Benasciutti and modified Fu–Cebon methods were recommended as being the most accurate [51].

The primary aim of this review is to develop a common theoretical and open-source-code framework for a side-by-side comparison of more than 20 spectral methods, including those introduced in recent years. This framework will help to advance and speed-up future spectral-domain vibration fatigue-damage-estimation research. In this review the spectral methods are also compared to the time-domain rainfall algorithm; the comparison is based on signals defined by the PSDs, representing typical response in structural dynamics: spectral width, background noise, close modes and number of modes. In addition, typical vibration profiles used in accelerated automotive tests are also considered. The reviewed methods are implemented in the supporting open-source Python package FLife [70]; the comparison is fully reproducible using the package documentation.

This manuscript is organized as follows. In Section 2 a brief theoretical background to random-process and uniaxial vibration-fatigue theory is presented. A detailed theoretical background of the spectral methods is given in Section 3. In Section 4, the spectral methods are compared for different PSD signals and for different fatigue parameters, followed by a discussion of the results in Section 5. The conclusions are drawn in Section 6.

## 2. Theoretical background

Vibration fatigue by spectral methods relates the theory of structural dynamics to high-cycle vibration fatigue [1]. To facilitate a fatigue-life estimation in the frequency-domain, a brief theoretical background to stochastic process theory and uniaxial vibration fatigue is presented in this section.

Frequency-domain spectral methods are of great interest for fatigue analysis since structural dynamics is described in the frequency domain. The response of a linear, time-invariant, multi-degree-of-freedom system to a stationary and Gaussian-distributed excitation is stationary and Gaussian [2]. The presented theory focuses on uniaxial vibration fatigue; a uniaxial stress state and a high-cycle load are assumed. For a more comprehensive study of vibration fatigue the reader is referred to the work of Slavič et al. [1].

### 2.1. Random process properties

For a uniaxial stationary Gaussian-distributed zero-mean random process  $X(t)$  the power spectral density (PSD) is typically used to define the process in the frequency domain. A frequent confusion and source of error are the different forms of PSD: a two-sided symmetrical spectrum  $S_{xx}(\omega)$  and one-sided spectrum  $W_{xx}(\omega)$  have their frequency axis in rad/s, where  $W_{xx}(\omega)=2 S_{xx}(\omega)$  for  $\omega > 0$ ,  $W_{xx}(\omega)=S_{xx}(\omega)$  for  $\omega = 0$ , and  $W_{xx}(\omega)=0$  for  $\omega < 0$ . Alternatively, a one-sided spectrum  $G_{xx}(f)$  with the frequency axis in Hz is often used and is related to the two-sided PSD as  $G_{xx}(f)=4 \pi S_{xx}(\omega=2 \pi f)$  [2]. Dependent on the PSD type, the general form of the  $i$ th spectral moment is defined as [36,71]:

$$m_i = \int_{-\infty}^{\infty} |\omega|^i S_{xx}(\omega) d\omega = \int_0^{\infty} \omega^i W_{xx}(\omega) d\omega = (2 \pi)^i \int_0^{\infty} f^i G_{xx}(f) df. \tag{1}$$

Even spectral moments coincide with the variance  $\sigma_x^2$  of the random process  $X(t)$  and the variance of its derivatives [36], for instance:

$$\sigma_x^2 = m_0, \quad \sigma_{\dot{x}}^2 = m_2, \quad \sigma_{\ddot{x}}^2 = m_4. \tag{2}$$

Based on spectral moments (1), the frequency of the positive slope zero crossing  $v_0^+$  and the expected peak frequency  $v_p$  are defined as [2]:

$$v_0^+ = \frac{1}{2\pi} \sqrt{\frac{m_2}{m_0}}, \quad v_p = \frac{1}{2\pi} \sqrt{\frac{m_4}{m_2}}. \tag{3}$$

To describe the spectral width of the random process the bandwidth parameter  $\alpha_i$  is defined as [71,72]:

$$\alpha_i = \frac{m_i}{\sqrt{m_0 m_{2i}}}, \tag{4}$$

where the most commonly used  $\alpha_2$ , known as the irregularity factor, represents the ratio of the positive slope zero crossing and expected peak frequency [71]. In general, for a narrowband process the irregularity factor approaches one, whereas it tends towards

zero with an increase of the frequency width of a random process. Alternatively, the spectral width parameter  $\epsilon$  is used by some researchers (close to zero for narrowband and close to one for broadband process) [40,73]:

$$\epsilon = \sqrt{1 - \alpha_2^2}. \tag{5}$$

Another established estimator is the Vanmarcke bandwidth parameter  $\epsilon_V$  [74]:

$$\epsilon_V = \sqrt{1 - \alpha_1^2}. \tag{6}$$

The most important distinction between narrowband and broadband random processes is manifested in their probability distribution of peaks. For a general broadband process  $X(t)$  Rice [75] provided the probability density function (PDF) of the peak amplitude  $p_p(x)$ :

$$p_p(x) = \frac{\sqrt{1 - \alpha_2^2}}{\sqrt{2\pi}\sigma_x} e^{-\frac{x^2}{2\sigma_x^2(1-\alpha_2^2)}} + \frac{\alpha_2 x}{\sigma_x^2} e^{-\frac{x^2}{2\sigma_x^2}} \Phi\left(\frac{\alpha_2 x}{\sigma_x \sqrt{1 - \alpha_2^2}}\right) \tag{7}$$

with  $\Phi(\cdot)$  being the standard normal cumulative distribution function:

$$\Phi(z) = \frac{1}{\sqrt{2\pi}} \int_{-\infty}^z e^{-\frac{t^2}{2}} dt. \tag{8}$$

### 2.2. Vibration-fatigue-life estimation

In vibration fatigue the stress-life approach is based on the S-N curve [1,68]:

$$s_a^k N = C, \tag{9}$$

where  $N$  is the number of cycles to failure at the stress amplitude  $s_a$ . The parameters  $C$  and  $k$  are the fatigue-strength coefficient and the fatigue-strength exponent, respectively. Given the stress time-history  $s(t)$ , the stress cycles must be extracted to estimate the fatigue life. The rainflow-counting algorithm [4,76] is adopted as it is accepted as the most reliable (out of many counting schemes that are available) [77]. The hypothesis of linear damage accumulation by Palmgren [6] and Miner [7] is employed to sum the damages due to individual stress cycles. For random processes it is customary to use the mathematical expectation (operator  $E[\cdot]$ ) of the fatigue damage, since the stress-cycle amplitudes are non-deterministic:

$$D = E\left[\sum_{i=1}^n \frac{1}{N(s_{a,i})}\right] = \frac{1}{C} E\left[\sum_{i=1}^n s_{a,i}^k\right] = \frac{\bar{n}}{C} E[s_a^k], \tag{10}$$

where  $\bar{n} = E[n]$  denotes the mean number of stress cycles counted in the time period  $T$ . The  $k$ th moment of the cycle-amplitude distribution  $p_a(s)$  is given as [73]:

$$E[s_a^k] = \int_0^\infty s^k p_a(s) ds \tag{11}$$

and can be obtained in both the time and frequency domains. In general, time-domain analysis is expensive in terms of computational time, and so vibration fatigue using spectral methods might be preferable [1]. In a frequency-domain fatigue analysis it is common to refer to the damage in terms of the damage rate or the damage per unit time, defined as [1,42]:

$$d = \frac{D}{T} = \nu_p C^{-1} \int_0^\infty s^k p_a(s) ds, \tag{12}$$

where for a stationary and Gaussian random process the expected peak frequency  $\nu_p$  (3) is used in place of  $\bar{n}/T$ .

### 2.3. Narrowband random process

In the case of a narrowband random process the cycle-amplitude distribution coincides with the peak-amplitude distribution (also, the frequency of the positive slope zero crossing  $\nu_0^+$  coincides with the expected peak frequency  $\nu_p$ ) and the Rice distribution (7) turns into the Rayleigh distributed amplitude PDF [78]:

$$p_{a,NB}(s) = \frac{s}{\sigma_s^2} e^{-\frac{s^2}{2\sigma_s^2}}, \tag{13}$$

where the variance  $\sigma_s^2$  of the load  $s(t)$  is obtained as the zeroth spectral moment (2). With the known cycle-amplitude distribution (13), the close form of the damage intensity (12) is given by Bendat [36,37] as:

$$d^{NB} = \nu_0^+ C^{-1} \left(\sqrt{2m_0}\right)^k \Gamma\left(1 + \frac{k}{2}\right), \tag{14}$$

where  $\Gamma(\cdot)$  denotes the Euler gamma function:

$$\Gamma(z) = \int_0^\infty t^{z-1} e^{-t} dt. \tag{15}$$

### 3. Spectral methods for a broadband random process

If a random process is considered narrowband, an exact solution for the damage intensity exists, Eq. (14). In contrast, for broadband process the solutions are devised only in an approximate form. This section discusses in detail the spectral methods for a fatigue life-estimation of broadband random processes; based on the damage estimation concept, the methods are arranged into four categories, as shown in Fig. 1.

#### 3.1. Narrowband correction factor

Using the narrowband formulation in the case of a broadband random process results in a conservative fatigue-life estimate [15]. Hence, numerous narrowband correction factors have been proposed. In accordance with the correction factor, the damage intensity assumes the following form:

$$d^{\text{method}} = \rho_{\text{method}} d^{\text{NB}}, \tag{16}$$

where  $\rho_{\text{method}}$  designates the method's correction factor and  $d^{\text{NB}}$  is defined with Eq. (14).

*Wirsching–Light method (1980).* Wirsching and Light [40] adapted the narrowband method with an empirically determined correction factor based on extensive Monte Carlo simulations:

$$\rho_{\text{WL}} = a(k) + [1 - a(k)] (1 - \epsilon)^{b(k)}, \tag{17}$$

dependent on the spectral width parameter  $\epsilon$  (5) and on the S-N curve's fatigue-strength exponent  $k$ . The terms  $a(k)$  and  $b(k)$  were determined as a best fit in numerical simulations for the fatigue-strength exponent  $k = 3, 4, 5$  and  $6$  with respect to the rainflow-counting method:

$$a(k) = 0.926 - 0.033 k, \quad b(k) = 1.587 k - 2.323. \tag{18}$$

*Ortiz–Chen method (1987).* The spectral method by Ortiz and Chen [41] introduces the generalized spectral bandwidth  $\beta$  to define the correction factor:

$$\rho_{\text{OC}} = \frac{\beta^k}{\alpha_2}, \tag{19}$$

where the generalized spectral bandwidth depends on the S-N curve's fatigue-strength exponent  $k$  [41,67]:

$$\beta = \sqrt{\frac{m_2 m_{2/k}}{m_0 m_{2/k+2}}}. \tag{20}$$

*Tovo–Benasciutti method (2002, 2005).* Based on the findings of Frenthal and Rychlik [79], Tovo reasoned that for a Gaussian random process the rainflow damage intensity  $d^{\text{RFC}}$  is always limited [14]:

$$d^{\text{RC}} \leq d^{\text{RFC}} \leq d^{\text{NB}}. \tag{21}$$

Rychlik [39] showed that the upper bound of the damage intensity is equal to the narrowband formula  $d^{\text{NB}}$ , whereas the lower bound, coincident with the range-count counting method in the time domain, has no exact analytical expression. Its approximation was adopted by Madsen [80]:

$$d^{\text{RC}} \cong v_p C^{-1} \left( \sqrt{2 m_0} \alpha_2 \right)^k \Gamma \left( 1 + \frac{k}{2} \right) = d^{\text{NB}} \alpha_2^{k-1}. \tag{22}$$

Tovo proposed a solution in a form of a linear combination between these two limits [14]:

$$d^{\text{TB}} = b d^{\text{NB}} + (1 - b) d^{\text{RC}} = [b + (1 - b) \alpha_2^{k-1}] d^{\text{NB}}, \tag{23}$$

from which the narrowband correction factor is revealed:

$$\rho_{\text{TB}} = b + (1 - b) \alpha_2^{k-1}. \tag{24}$$

The authors suggested two formulations for the coefficient  $b$ :

$$b^{\text{TB}_1} = \min \left\{ \frac{\alpha_1 - \alpha_2}{1 - \alpha_1}, 1 \right\}, \quad \text{see: [14]}, \tag{25}$$

$$b^{\text{TB}_2} = \frac{(\alpha_1 - \alpha_2) [1.112 (1 + \alpha_1 \alpha_2 - (\alpha_1 + \alpha_2)) e^{2.11 \alpha_2} + (\alpha_1 - \alpha_2)]}{(\alpha_2 - 1)^2}, \quad \text{see: [43]}, \tag{26}$$

where Eq. (26) was obtained based on the results from numerical simulations considering different broadband spectra with various combinations of  $\alpha_1$  and  $\alpha_2$ . Moreover, the Tovo-Benasciutti method applies the same linear combination as in Eq. (23) to obtain the stress amplitude PDF [14,65] as:

$$p_{\text{a,TB}}(s) = b p_{\text{LCC}}(s) + (1 - b) p_{\text{RC}}(s) = b \alpha_2 \frac{s}{\sigma_x^2} e^{\frac{-s^2}{2\sigma_x^2}} + (1 - b) \frac{s}{\sigma_x^2 \alpha_2^2} e^{\frac{-s^2}{2\alpha_2^2 \sigma_x^2}}, \tag{27}$$

where  $p_{\text{LCC}}(s)$  and  $p_{\text{RC}}(s)$  denote level-crossing counting and range counting marginal amplitude density, respectively. In addition, the authors have extended the method for the non-Gaussian random loads [27].

$\alpha_{0.75}$  method (2004). As observed by Lutes et al. [72] there is a possible correlation of the rainflow fatigue damage on some particular bandwidth parameters (4), i.e. on  $\alpha_{0.75}$ . On a purely empirical basis, Benasciutti and Tovo [42] suggested a simple but effective formulation of the narrowband correction factor, dependent only on the  $\alpha_{0.75}$  bandwidth parameter:

$$\rho_{BT} = \alpha_{0.75}^2. \tag{28}$$

### 3.2. Rainflow PDF approximation

Instead of applying the narrowband correction factor the damage intensity can be obtained by means of an integral over the stress-cycle amplitudes (12). Hence, the cycle amplitude PDF is a prerequisite. This subsection discusses the spectral methods that approximate the rainflow-cycle amplitude PDF of a general broadband process.

*Dirlik method (1985)*. Dirlik [44] devised an empirical closed-form formula for the rainflow-cycle amplitude PDF based on extensive numerical simulations. Even if the aims of Dirlik’s research were oriented to finding an appropriate cycle amplitude distribution for the PSD of bimodal form, his formula returns results in good agreement with the rainflow fatigue damage in the case of broadband processes [15]. The proposed method models the cycle-amplitude probability by combining one exponential and two Rayleigh probability densities:

$$p_{a,DK}(s) = \frac{1}{\sqrt{m_0}} \left( \frac{G_1}{Q} e^{-\frac{Z}{Q}} + \frac{G_2 Z}{R^2} e^{-\frac{Z^2}{R^2}} + G_3 Z e^{-\frac{Z^2}{2}} \right), \tag{29}$$

where  $Z$  designates the normalized amplitude:

$$Z = \frac{s}{\sqrt{m_0}}. \tag{30}$$

The parameters  $G_1, G_2, G_3, R, Q$  and the mean frequency  $x_m$  are determined as [65]:

$$\begin{aligned} G_1 &= \frac{2(x_m - \alpha_2^2)}{1 + \alpha_2^2}, & G_2 &= \frac{1 - \alpha_2 - G_1 + G_1^2}{1 - R}, \\ G_3 &= 1 - G_1 - G_2, & R &= \frac{\alpha_2 - x_m - G_1^2}{1 - \alpha_2 - G_1 + G_1^2}, \\ Q &= \frac{1.25(\alpha_2 - G_3 - G_2 R)}{G_1}, & x_m &= \frac{m_1}{m_0} \left( \frac{m_2}{m_4} \right)^{\frac{1}{2}}. \end{aligned} \tag{31}$$

The closed-form expression for the damage intensity is defined as [65]:

$$d^{DK} = v_p C^{-1} m_0^{k/2} \left[ G_1 Q^k \Gamma(1 + k) + \left( \sqrt{2} \right)^k \Gamma\left(1 + \frac{k}{2}\right) (G_2 |R|^k + G_3) \right]. \tag{32}$$

*Zhao–Baker method (1992)*. Introduced by Zhao and Baker [45], this method gives the rainflow-cycle amplitude distribution in the form of a linear combination of the Weibull and Rayleigh PDF:

$$p_{a,ZB}(Z) = w \alpha \beta Z^{\beta-1} e^{-\alpha Z^\beta} + (1 - w) Z e^{-\frac{Z^2}{2}}, \tag{33}$$

where  $Z$  is the normalized amplitude (30). The weighting coefficient  $w$  is defined as:

$$w = \frac{1 - \alpha_2}{1 - \sqrt{\frac{2}{\pi}} \Gamma\left(1 + \frac{1}{\beta}\right) \alpha^{-1/\beta}} \tag{34}$$

and  $\alpha$  and  $\beta$  are the Weibull distribution coefficients:

$$\alpha = 8 - 7 \alpha_2, \tag{35}$$

$$\beta = \begin{cases} 1.1; & \alpha_2 < 0.9 \\ 1.1 + 9(\alpha_2 - 0.9); & \alpha_2 \geq 0.9 \end{cases} \tag{36}$$

It has been observed that for low values of the fatigue-strength exponent  $k$  the vibration fatigue damage is better related to  $\alpha_{0.75}$  than to the  $\alpha_2$  bandwidth parameter [72]. For that reason Zhao and Baker devised an improved procedure for determining the Weibull distribution coefficient  $\alpha$  (35) in the case of  $k=3$ . For details, the reader is referred to the original research [45].

For the value  $\alpha_2 < 0.13$ , the coefficient  $w$  becomes greater than 1, which is an erroneous result for this specific spectral method. The Zhao-Baker method should therefore be avoided for processes with such an (uncommonly) low value of  $\alpha_2$ . Furthermore, the method was tuned in simulations with a fatigue-strength exponent in the range  $2 \leq k \leq 6$  and should be used carefully otherwise.

The closed-form expression for the Zhao-Baker method is given as [45,65]:

$$d^{ZB} = v_p C^{-1} m_0^{k/2} \left[ w \alpha^{-\frac{k}{\beta}} \Gamma\left(1 + \frac{k}{\beta}\right) + (1 - w) 2^{k/2} \Gamma\left(1 + \frac{k}{2}\right) \right]. \tag{37}$$

*Park method (2014).* In 2014, Park et al. [46] presented a spectral method where they combined three distributions to approximate the rainflow-cycle amplitude PDF: a Rayleigh, a standard Rayleigh and a half-Gaussian distribution:

$$p_{a,PK}(Z) = c_{R_1} \frac{Z}{\sigma_{R_1}^2} e^{-\frac{Z^2}{2\sigma_{R_1}^2}} + c_{R_2} Z e^{-\frac{Z^2}{2}} + c_G \frac{2}{\sqrt{2\pi}\sigma_G} e^{-\frac{Z^2}{2\sigma_G^2}}, \tag{38}$$

where  $Z$  stands for the normalized amplitude (30). To determine the unknown coefficients, the normalized moments of the rainflow stress range distribution were utilized, as introduced by Dirlik [44]:

$$M_{RR}(n) = \frac{\int_0^\infty z^n p_{RFC}(z) dz}{\int_0^\infty z^{n+1} e^{-\frac{z^2}{2}} dz}. \tag{39}$$

The moments  $M_{RR}(n)$  up to  $n=3$  are approximated using the bandwidth parameter  $\alpha_i$  (4), such as:

$$M_{RR}(1) \approx \alpha_2, \quad M_{RR}(2) \approx \alpha_{0.95} \alpha_{1.97}, \quad M_{RR}(3) \approx \alpha_{0.54} \alpha_{0.93} \alpha_{1.95}. \tag{40}$$

Inserting the proposed PDF (38) into Eq. (39) for  $n=1, 2, 3$ , a system of four equations with four unknowns is formed (the result of the parametric simulations is the approximation  $\sigma_{R_1} \approx \alpha_2$ ), yielding the distribution coefficients:

$$\begin{aligned} c_{R_1} &= \frac{M_{RR}(2) - M_{RR}(3)}{\sigma_{R_1}^2 (1 - \sigma_{R_1})}, & \sigma_{R_1} &\approx \alpha_2, \\ c_{R_2} &= \frac{-\sigma_{R_1} M_{RR}(2) + M_{RR}(3)}{1 - \sigma_{R_1}}, & c_G &= 1 - c_{R_1} - c_{R_2}, \\ \sigma_G &= \frac{\sqrt{\pi} \Gamma(1.5)}{c_G \Gamma(1)} \left( M_{RR}(1) - c_{R_1} \sigma_{R_1} - c_{R_2} \right). \end{aligned} \tag{41}$$

The close-form expression for the damage intensity is given as:

$$\begin{aligned} d^{PK} &= v_p C^{-1} (\sqrt{2m_0})^k \left[ \frac{c_G}{\sqrt{\pi}} \sigma_G^k \Gamma\left(\frac{1+k}{2}\right) \right. \\ &\quad \left. + c_{R_1} \sigma_{R_1}^k \Gamma\left(1 + \frac{k}{2}\right) + c_{R_2} \Gamma\left(1 + \frac{k}{2}\right) \right]. \end{aligned} \tag{42}$$

*Jun–Park method (2020).* Jun and Park [47] proposed a spectral method that is similar to the Park method, with one essential distinction: the rainflow-cycle amplitude PDF is approximated with an additional exponential term:

$$\begin{aligned} p_{a,JP}(Z) &= Q_c \left[ D_1 \frac{1}{\sigma_E} e^{-\frac{Z}{\sigma_E}} + D_2 \frac{Z}{\sigma_R^2} e^{-\frac{Z^2}{2\sigma_R^2}} \right. \\ &\quad \left. + D_3 Z e^{-\frac{Z^2}{2}} + D_4 \frac{2}{\sqrt{2\pi}\sigma_H} e^{-\frac{Z^2}{2\sigma_H^2}} \right], \end{aligned} \tag{43}$$

where  $Z$  denotes the normalized variance (30). Also, a correction factor  $Q_c$  is introduced to further improve the accuracy of the proposed method:

$$\begin{aligned} Q_c(\alpha_1, \alpha_2) &= 0.903 - 0.28(\alpha_1 - \alpha_2) + 4.448(\alpha_1 - \alpha_2)^2 \\ &\quad - 15.739(\alpha_1 - \alpha_2)^3 + 19.57(\alpha_1 - \alpha_2)^4 - 8.054(\alpha_1 - \alpha_2)^5 \\ &\quad + 1.013\alpha_2 - 4.178\alpha_2^2 + 8.362\alpha_2^3 - 7.993\alpha_2^4 + 2.886\alpha_5. \end{aligned} \tag{44}$$

Note that the correction factor scales the PDF, although Jung and Park state that it makes the proposed PDF model very close to the RFC distribution [47]. The correction factor should therefore be interpreted in terms of the damage correction. The unknowns of the proposed PDF are determined using the normalized moments of the rainflow stress range distribution  $M_{RR}(n)$ , defined by Eq. (39). The first four moments are approximated with the bandwidth parameter  $\alpha_i$  (4) and the special bandwidth parameter  $\mu_k$  (not to be confused with the fatigue-strength exponent  $k$ ) [47]:

$$\mu_k = \frac{m_{k+0.01}}{\sqrt{m_{0.01} m_{2k+0.01}}} \tag{45}$$

as follows:

$$M_{RR}(1) \approx \rho \mu_1^{-0.96}, \quad M_{RR}(2) \approx \rho \mu_1^{-0.02}, \quad M_{RR}(3) \approx \rho \mu_{0.52}, \quad M_{RR}(4) \approx \rho \mu_{0.55}, \tag{46}$$

where  $\rho = \alpha_1^{-1.1} \alpha_2^{0.9}$ . Combining  $M_{RR}(n)$  with the proposed PDF, seven coefficients ( $D_1$ ,  $\sigma_E$  and  $\sigma_R$  are determined according to Dirlik [44] and Benasciutti [81], respectively) can be obtained as:

$$\begin{aligned} D_1 &= \frac{2(\alpha_1 \alpha_2 - \alpha_2^2)}{1 + \alpha_2^2}, \quad D_2 = \frac{M_{RR}(2) - M_{RR}(3)}{\sigma_R^2 (1 - \sigma_R)}, \quad D_3 = \frac{-\sigma_R M_{RR}(2) + M_{RR}(3)}{1 - \sigma_R}, \\ D_4 &= 1 - D_1 - D_2 - D_3, \quad \sigma_E = \frac{1}{A_1 D_1} (M_{RR}(1) - D_2 \sigma_R - D_3 - B_1 D_4 \sigma_H), \end{aligned}$$

$$\sigma_R \approx \alpha_2, \quad \sigma_H = \frac{1}{B_1 D_4} (M_{RR}(1) - D_1^2 - D_2 \sigma_R - D_3), \tag{47}$$

where  $A_n = \frac{\Gamma(1+n)}{\sqrt{2\pi} \Gamma(1+n/2)}$  and  $B_n = \frac{\Gamma((1+n)/2)}{\sqrt{\pi} \Gamma(1+n/2)}$ . The close-form expression for the damage intensity is given as:

$$d^{JP} = Q_c v_p C^{-1} (\sqrt{2 m_0})^k \left[ \frac{D_1}{\sqrt{2}^k} \sigma_E^k \Gamma(1+k) + D_2 \sigma_R^k \Gamma\left(1 + \frac{k}{2}\right) + D_3 \Gamma\left(1 + \frac{k}{2}\right) + \frac{D_4}{\sqrt{\pi}} \sigma_H^k \Gamma\left(\frac{1+k}{2}\right) \right]. \tag{48}$$

### 3.3. Combined fatigue damage - cycle damage combination

Special cases of the broadband random processes are the multimodal processes, which have a spectral density formed by the superposition of two or more well-separated narrowband contributions. Such spectra are typical of the loading responses observed in offshore platforms under waveloadings or in automotive chassis components [51]. By analyzing these processes in the time domain, a rainflow algorithm extracts the clearly distinguishable classes of stress cycles; a pioneering work by Jiao and Moan [48] on bimodal fatigue analysis showed that bimodal process in the time domain exhibits small-amplitude and large-amplitude cycles. Since structural components are often subjected to the combined effect of one low-frequency and one high-frequency load, bimodal research gained attention and several publications tried to improve the bimodal-based research’s accuracy and efficiency.

*Bimodal random process.* This paragraph extends the theoretical background in terms of the bimodal random process. If the process  $X(t)$  is composed of the low-frequency (LF) component  $X_{LF}(t)$  and the high-frequency (HF) component  $X_{HF}(t)$  (which are independent):

$$X(t) = X_{LF}(t) + X_{HF}(t), \tag{49}$$

the PSD can be defined in terms of both components:

$$W_{xx}(\omega) = W_{xx,LF}(\omega) + W_{xx,HF}(\omega), \tag{50}$$

as depicted in Fig. 2, together with the corresponding time–history realization. Accordingly, the  $i$ th spectral moment (1) is rewritten as:

$$m_i = \int_0^\infty \omega^i [W_{xx,LF}(\omega) + W_{xx,HF}(\omega)] d\omega = m_{i,LF} + m_{i,HF}, \tag{51}$$

where  $m_{i,LF}$  and  $m_{i,HF}$  denote the  $i$ th spectral moments of  $X_{LF}(t)$  and  $X_{HF}(t)$ , respectively. The frequency of the positive slope zero crossing and the expected peak frequency (3) are revised to be congruent with the LF and HF components:

$$v_{0,mode}^+ = \frac{1}{2\pi} \sqrt{\frac{m_{2,mode}}{m_{0,mode}}}, \quad v_{p,mode} = \frac{1}{2\pi} \sqrt{\frac{m_{4,mode}}{m_{2,mode}}}, \tag{52}$$

where the subscript ‘mode’ denotes LF and HF. When inspecting the random process in the time domain, clearly distinguishable small-amplitude and large-amplitude cycles can be observed, as shown in Fig. 2(b). The intricate dependence of the cycle-amplitude distribution and cycle count on the bimodal PSD has been thoroughly researched [48,50,52]; once the cycle-amplitude distribution and cycle count are formulated, the damage corresponding to the small-amplitude and large-amplitude cycles can be estimated. The combined fatigue damage is then taken as the sum of both contributions:

$$d^{method} = d_S + d_L, \tag{53}$$

where the superscript ‘method’ denotes the spectral method used to formulate the damage intensities due to the small-amplitude cycles  $d_S$  and the large-amplitude cycles  $d_L$ .

*Jiao–Moan method (1990).* Research by Jiao and Moan [48] on bimodal fatigue analysis showed that bimodal processes in the time domain exhibit clearly distinguishable small- and large-amplitude cycles. Accordingly, the total fatigue damage can be expressed as the sum of the respective damages, Eq. (53), where the small-amplitude cycles are attributed solely to the HF process, as depicted in Fig. 2(b). The small-amplitude cycle damage intensity  $d_S$  is thus evaluated through a narrowband approximation (14), utilizing the frequency of the small-amplitude cycles  $v_{0,HF}^+$  and the variance of the HF component,  $m_{0,HF}$ . It should be noted that Jiao and Moan [48] investigated the fatigue for a random process with unit variance,  $m_0 = 1$ .

To evaluate the damage intensity due to large-amplitude cycles  $d_L$ , which is dominated by the envelope of the superimposed LF and HF components, the damage-accumulation model (12) is used. The large-amplitude cycle amplitude PDF is determined with the convolution of two Rayleigh distributions:

$$p_{a,L}(s) = p_{R,HF}(s) * p_{R,LF}(s) = \int_0^\infty p_{R,HF}(r) p_{R,LF}(s-r) dr \\ = m_{0,LF} s e^{-\frac{s^2}{2m_{0,LF}}} + m_{0,HF} s e^{-\frac{s^2}{2m_{0,HF}}} \\ + \sqrt{2\pi m_{0,LF} m_{0,HF}} (s^2 - 1) e^{-\frac{s^2}{2}} \left[ \Phi\left(\sqrt{\frac{m_{0,LF}}{m_{0,HF}}} s\right) + \Phi\left(\sqrt{\frac{m_{0,HF}}{m_{0,LF}}} s\right) - 1 \right], \tag{54}$$

where the Rayleigh distributions  $p_{R_{HF}}(s)$  and  $p_{R_{LF}}(s)$  are defined with Eq. (13) and  $\Phi(\cdot)$  denotes the standard normal cumulative distribution function (8). The frequency of the large-amplitude cycles is approximated by the mean upcrossing rate:

$$v_{0,L}^+ = m_{0,LF} v_{0,LF}^+ \sqrt{1 + \frac{m_{0,HF}}{m_{0,LF}} \left( \frac{v_{0,HF}^+}{v_{0,LF}^+} \epsilon_v \right)^2} \tag{55}$$

with the Vanmarcke bandwidth parameter  $\epsilon_v$  defined with Eq. (6).

Jiao and Moan’s method includes the damage contribution of the large-amplitude cycles only when the LF component is important (i.e., only when  $m_{0,LF}$  is large) and approximates Eq. (54) as:

$$p_{a,L}(s) \approx \left( m_{0,LF} - \sqrt{m_{0,LF} m_{0,HF}} \right) s e^{-\frac{s^2}{2m_{0,LF}}} + \sqrt{2\pi m_{0,LF} m_{0,HF}} (s^2 - 1) e^{-\frac{s^2}{2}}. \tag{56}$$

Considering the proposed large-amplitude cycle amplitude PDF (56), the closed-form expression for the damage intensity can be given in the form of a damage-correction factor (16) [51]:

$$d^{JM} = \left( \frac{v_{0,L}^+}{v_0^+} \left[ m_{0,LF}^{\frac{k}{2}+2} \left( 1 - \sqrt{\frac{m_{0,HF}}{m_{0,LF}}} \right) + \sqrt{\pi m_{0,LF} m_{0,HF}} \frac{k \Gamma\left(\frac{k+1}{2}\right)}{\Gamma\left(1 + \frac{k}{2}\right)} \right] + \frac{v_{0,HF}^+}{v_0^+} m_{0,HF} \right) d^{NB} = \rho_{JM} d^{NB}. \tag{57}$$

*Sakai–Okamura method (1995).* Sakai and Okamura [49] assumed that in the case of a bimodal load, the total damage can be expressed directly as the sum of two narrowband damages, effected by the LF and HF components. The close-form solution provided by Sakai and Okamura is given as:

$$d^{SO} = \frac{2^{k/2}}{2\pi C} \Gamma\left(1 + \frac{k}{2}\right) \left[ m_{0,LF}^{(k-1)/2} m_{2,LF}^{1/2} + m_{0,HF}^{(k-1)/2} m_{2,HF}^{1/2} \right]. \tag{58}$$

This method does not account for the interactions between the LF and HF components.

*Fu–Cebon method (2000).* Fu and Cebon [50] investigated bimodal fatigue with similar reasoning to Jiao and Moan [48], although their approach differs in the definition of the frequency of small- and large-amplitude cycles. The damage intensity due to large-amplitude cycles is evaluated with the damage-accumulation model (12), where the cycles are approximated by the superposition of the LF and HF components. The large-amplitude cycle distribution is expressed by the convolution integral:

$$p_{a,L}(s) = \frac{1}{m_{0,L} m_{0,H}} e^{-\frac{s^2}{2m_{0,H}}} \int_0^s (s y - y^2) e^{-U y^2 + V s y} dy \tag{59}$$

with the constants  $U$  and  $V$ :

$$U = \frac{1}{2m_{0,LF}} + \frac{1}{2m_{0,HF}}, \quad V = \frac{1}{m_{0,HF}}. \tag{60}$$

Fu and Cebon claim that Eq. (59) has no closed-form solution and requires numerical integration; however, Benasciutti and Tovo [51] reasoned that the presented distribution coincides with the large-amplitude cycle distribution in the Jiao-Moan method (54), since the definition of the large-amplitude cycle is the same for both methods. The average frequency of the large-amplitude cycles is defined as the frequency of the positive slope zero crossing of the LF component,  $v_{0,LF}^+$ .

The damage intensity associated with the small-amplitude cycles is obtained with the narrowband formulation (14), as small-amplitude cycles are dependent only on the HF component and are considered Rayleigh distributed. However, Fu and Cebon assumed that the frequency of the small-amplitude cycles is affected by both components: if the total number of cycles is determined by the HF component’s frequency of the positive slope zero crossing  $v_{0,HF}^+$  and the random process length  $T$ , then the number of small-amplitude cycles equals  $(v_{0,HF}^+ - v_{0,LF}^+) T$ , i.e., the frequency of the small-amplitude cycles is  $v_{0,HF}^+ - v_{0,LF}^+$ .

*Modified Fu–Cebon method (2004).* Benasciutti and Tovo [51] proposed a slight modification to the Fu-Cebon [50] method with regard to the frequency of the small- and large-amplitude cycles. The large-amplitude cycle frequency is taken to be  $v_{0,L}^+$ , as defined in the Jiao-Moan method with Eq. (55), and the small-amplitude cycle frequency is equal to the difference between the frequency of the positive slope zero crossing of the HF component and the large cycle frequency, i.e.  $v_{0,HF}^+ - v_{0,L}^+$ . As in the Fu-Cebon method, the damage intensity due to the small-amplitude cycles is evaluated with the narrowband approximation (14) and the damage intensity due to the large-amplitude cycles with the damage-accumulation model (12).

Table 1 summarizes the Jiao-Moan, Fu-Cebon and modified Fu-Cebon methods and emphasizes their differences.

*Low’s bimodal method (2010).* Low’s bimodal method [52] involves two important effects regarding small- and large-amplitude cycles. Firstly, rather than equal, as assumed by Jiao and Moan [48], the small-amplitude cycles were demonstrated to be smaller than the HF process amplitude, since the presence of the LF component reduces their amplitude (Effect A) [52]. The damage intensity

**Table 1**  
Summary of Jiao-Moan, Fu-Cebon and modified Fu-Cebon spectral methods.

Spectral method	$d_S$ , narrowband approximation formula, Eq. (14)		$d_L$ , damage accumulation model, Eq. (12)	
	Frequency	Variance	Frequency	PDF
Jiao-Moan	$v_{0,HF}^+ - v_{0,LF}^+$	$m_{0,HF}$	$v_{0,L}^+$	$p_{a,L}$ , Eqs. (54), (56)
Fu-Cebon	$v_{0,HF}^+ - v_{0,LF}^+$	$m_{0,HF}$	$v_{0,LF}^+$	$p_{a,L}$ , Eqs. (54), (59)
Modified Fu-Cebon	$v_{0,HF}^+ - v_{0,L}^+$	$m_{0,HF}$	$v_{0,L}^+$	$p_{a,L}$ , Eq. (54)

due to the small-amplitude cycles is given as:

$$d_S = \frac{v_{0,HF}^+ - v_{0,LF}^+}{C} \int_0^\infty \int_{\frac{\pi}{4\beta}}^{\frac{\pi}{2}} \int_{\epsilon(r_{LF}, \phi)}^\infty [r_{HF} - \epsilon(r_{LF}, \phi)]^k p_{R_{HF}}(r_{HF}) p_\phi(\phi) p_{R_{LF}}(r_{LF}) dr_{HF} d\phi dr_{LF}, \tag{61}$$

where the corresponding cycle occurrence rate  $v_{0,HF}^+ - v_{0,LF}^+$  is according to Fu and Cebon [50]. In Eq. (61)  $R_{LF}$  and  $R_{HF}$  denote the Rayleigh distributed (13) stress amplitude of the LF and HF components, respectively. The decrease of the small-amplitude cycles is dependent on the LF component and the phase angle  $\phi$ :

$$\epsilon(r_{LF}, \phi) = \frac{\pi}{2\beta} r_{LF} \sin \phi, \tag{62}$$

where  $\beta$  denotes the ratio of the HF and LF component's frequency of positive slope zero crossing (52) and the phase angle  $\phi$  follows a uniform distribution [52]:

$$\beta = \frac{v_{0,HF}^+}{v_{0,LF}^+}, \tag{63}$$

$$p_\phi(\phi) = \left(\frac{\pi}{2} - \frac{\pi}{4\beta}\right)^{-1}, \quad \frac{\pi}{4\beta} \leq \phi \leq \frac{\pi}. \tag{64}$$

Secondly, the amplitude of the large-amplitude cycles is smaller than the direct addition of the LF and HF process amplitudes (Effect B) [52], since the peaks of the component processes do not occur at the same time. The damage intensity due to the large-amplitude cycles is formulated as:

$$d_L = \frac{v_{0,LF}^+}{C} \int_0^\infty \int_0^\infty \int_0^\pi [R_l(r_{LF}, r_{HF}, \psi)]^k p_\psi(\psi) p_{R_{HF}}(r_{HF}) p_{R_{LF}}(r_{LF}) d\psi dr_{HF} dr_{LF}, \tag{65}$$

where  $R_l$  is a function of three independent random variables: the Rayleigh distributed (13) stress amplitudes  $R_{LF}$  and  $R_{HF}$  and the uniformly distributed phase parameter  $\Psi$ . Two cosine functions are used to modify  $R_{LF}$  and  $R_{HF}$ :

$$R_l(r_{LF}, r_{HF}, \psi) = r_{LF} \cos(c(r_{LF}, r_{HF}) \psi) + r_{HF} \cos((\beta c(r_{LF}, r_{HF}) - 1) \psi), \tag{66}$$

$$c(r_{LF}, r_{HF}) = \frac{r_{HF} \beta}{r_{LF} + r_{HF} \beta^2}, \tag{67}$$

$$p_\psi(\psi) = \frac{1}{\pi}, \quad 0 \leq \psi \leq \pi. \tag{68}$$

The evaluation of the damage intensity due to the small-amplitude cycles (61) and large-amplitude cycles (65) requires a triple integration over three random variables, namely the HF and LF process amplitudes and a phase angle. However, the innermost integral of both equations can be evaluated analytically following a series expansion of the integrands [52], resulting in a reduction of the numerical integration to two dimensions.

*Low method (2014).* In 2014 Low [53] devised a simple and practical formula for fatigue-life prediction in the case of a bimodal Gaussian process. In his work, Low formulated a correction factor for the narrowband approximation, also viewed as the Rayleigh ratio [71]. Without a loss of generality, the total variance of the random process is normalized to unity [53]:

$$\sigma_{X_{LF}}^2 + \sigma_{X_{HF}}^2 = 1. \tag{69}$$

Considering the narrowband correction factor's form (16), the damage intensity is formulated as:

$$d^{Low} = \frac{L(\sigma_{X_{HF}}^2, \beta, k)}{\sqrt{1 - \sigma_{X_{HF}}^2 + \beta^2 \sigma_{X_{HF}}^2}} d^{NB}, \tag{70}$$

where  $L(\sigma_{X_{HF}}^2, \beta, k)$  denotes the LF damage ratio [53] and is approximated on the basis of a numerical simulation by minimizing the RMS error between the predicted damage and the rainflow-counting simulation results:

$$\begin{aligned} L &= \left[ b_1 \sigma_{X_{HF}} + b_2 \sigma_{X_{HF}}^2 - (b_1 + b_2) \sigma_{X_{HF}}^3 + \sigma_{X_{HF}}^k \right] (\beta - 1) + 1, \\ b_1 &= (1.111 + 0.7421 k - 0.0724 k^2) \beta^{-1} + (2.403 - 2.483 k) \beta^{-2}, \\ b_2 &= (-10.45 + 2.65 k) \beta^{-1} + (2.607 + 2.63 k - 0.0133 k^2) \beta^{-2}. \end{aligned} \tag{71}$$

The approximation is valid for  $3 \leq \beta < \infty$ ,  $[0 \leq \sigma_{HF}^2 \leq 1]$  and  $3 \leq k \leq 8$ . In Eqs. (70) and (71) the parameters  $\beta$ ,  $\sigma_{X_{HF}}^2$  and  $k$  are the ratio of frequencies of the positive slope zero crossing (63), the variance of the high-frequency component and the fatigue-strength exponent (9), respectively.

**Gao–Moan method (2008).** Gao and Moan [54] proposed a fatigue-damage combination method that estimates the cycle probabilities by combining three narrowband processes as:

$$X(t) = X_{LF}(t) + X_{MF}(t) + X_{HF}(t), \tag{72}$$

$$W_{xx}(\omega) = W_{xx,LF}(\omega) + W_{xx,MF}(\omega) + W_{xx,HF}(\omega), \tag{73}$$

where the subscripts LF, MF and HF denote the low-, middle- and high-frequency components, respectively. Each of them is Rayleigh distributed with the respective variance of  $m_{0,LF}$ ,  $m_{0,MF}$  and  $m_{0,HF}$ , expressed with the spectral moment as:

$$m_i = \int_0^\infty \omega^i [W_{xx,LF}(\omega) + W_{xx,MF}(\omega) + W_{xx,HF}(\omega)] d\omega = m_{i,LF} + m_{i,MF} + m_{i,HF}. \tag{74}$$

The proposed method is based on a bimodal fatigue analysis by Jiao and Moan [48] and assumes the total damage as the sum of individual damages due to small-, medium- and large-amplitude cycles:

$$d^{GM} = d_S + d_M + d_L. \tag{75}$$

As in the Jiao–Moan method, small-amplitude cycles are formed due to the HF component and the corresponding damage intensity  $d_S$  is evaluated with the narrowband approximation formula (14). Middle-amplitude cycles are formed due to the superposition of the MF and HF components and, analogously, the large-amplitude cycles are attributed to the superposition of the HF, MF and LF components of the random process, as depicted in Fig. 3(b). The damage-accumulation model (12) is used to evaluate the damage intensities  $d_M$  and  $d_L$ , where the expected peak frequencies are approximated as:

$$v_{0,M}^+ = \sqrt{m_{2,HF} \epsilon_{v,HF}^2 + m_{2,MF}} \frac{\sigma_{MF}}{(\sigma_{HF}^2 + \sigma_{MF}^2)}, \tag{76}$$

$$\begin{aligned} v_{0,L}^+ &= \sqrt{m_{2,HF} \epsilon_{v,HF}^2 + m_{2,MF} \epsilon_{v,MF}^2 + m_{2,LF}} \\ &\times \left[ \frac{2 \sigma_{LF} \sqrt{\sigma_{HF}^2 + \sigma_{MF}^2 + \sigma_{LF}^2} - \pi \sigma_{HF} \sigma_{MF}}{2 \left( \sqrt{\sigma_{HF}^2 + \sigma_{MF}^2 + \sigma_{LF}^2} \right)^3} \right. \\ &\left. + \frac{2 \sigma_{HF} \sigma_{MF} \arctan \left( \frac{\sigma_{HF} \sigma_{MF}}{\sigma_{LF} \sqrt{\sigma_{HF}^2 + \sigma_{MF}^2 + \sigma_{LF}^2}} \right)}{2 \left( \sqrt{\sigma_{HF}^2 + \sigma_{MF}^2 + \sigma_{LF}^2} \right)^3} \right]. \end{aligned} \tag{77}$$

In Eqs. (76) and (77) the  $\epsilon_{v,MF}$  and  $\epsilon_{v,HF}$  are the Vanmarcke parameters (6) for the MF and HF components of the random process, respectively. The medium- and large-amplitude cycle probabilities are derived by means of the convolution integral:

$$p_{a,M}(s) = \int_0^\infty p_{a,HF}(S) p_{a,MF}(s - S) dS, \tag{78}$$

$$p_{a,L}(s) = \int_0^\infty p_{a,M}(S) p_{a,LF}(s - S) dS, \tag{79}$$

where  $p_{a,HF}$ ,  $p_{a,MF}$  and  $p_{a,LF}$  are the cycle amplitude PDF for the respective narrowband random processes (13). Gao and Moan used Hermite integration to perform the convolution and obtain the PDF for the combination of Rayleigh random variables [54].

It is possible to generalize the trimodal approach to an arbitrary broadband random process that must first have its spectrum split into three parts according to some criterion. Gao and Moan [54] suggest the division using the criterion of equal area under the PSD curve. Each of the parts then takes the role of one of the processes –  $X_{LF}(t)$ ,  $X_{MF}(t)$  and  $X_{HF}(t)$ .

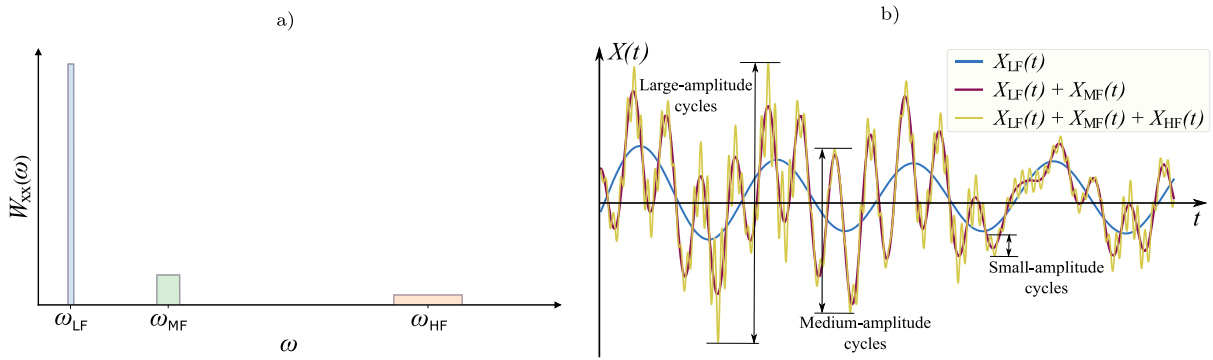


Fig. 3. Trimodal random process; (a) PSD, (b) time history and three distinct cycle categories: small-, medium- and large-amplitude cycles.

### 3.4. Combined fatigue damage - narrowband damage combination

The fatigue-damage combination form is convenient for practical applications because the combined fatigue damage is expressed as an explicit form of individual damages. Provided that the broadband stress spectrum is decomposed into a set of narrow-band spectral contributions, the classical narrowband formulation can be used to obtain the individual damages. Because the damage is nonlinearly dependent on stress, a direct sum of the individual damage contributions will underestimate the total damage.

*Lotsberg method (2005)*. Lotsberg [57] presented a method for a fatigue-damage combination as a nonlinear combination of the LF and HF damage contributions:

$$d^{LB} = d^{NB,HF} \left( 1 - \frac{v_{0,LF}^+}{v_{0,HF}^+} \right) + v_{0,LF}^+ \left[ \left( \frac{d^{NB,HF}}{v_{0,HF}^+} \right)^{\frac{1}{k}} + \left( \frac{d^{NB,LF}}{v_{0,LF}^+} \right)^{\frac{1}{k}} \right]^k, \tag{80}$$

where  $d^{NB,LF}$  and  $d^{NB,HF}$  are obtained by a narrowband formulation (14), associated with the LF and HF components, respectively. The frequency of the positive zero slope crossing for both components is defined by Eq. (52). Lotsberg’s formula is widely used in DNV specifications [82,83].

*Huang–Moan method (2006)*. Huang and Moan [58] proposed a method that combines damage due to the LF and HF components in a nonlinear way:

$$d^{HM} = \frac{\left( \left( \frac{d^{NB,LF}}{v_{0,LF}^+} \right)^{\frac{2}{k}} + \left( \frac{d^{NB,LF}}{v_{0,LF}^+} \right)^{\frac{2}{k}} \right)^{\frac{k-2}{2}} \left[ \left( v_{0,LF}^+ \right)^2 \left( \frac{d^{NB,LF}}{v_{0,LF}^+} \right)^{\frac{2}{k}} + \left( v_{0,HF}^+ \right)^2 \left( \frac{d^{NB,HF}}{v_{0,HF}^+} \right)^{\frac{2}{k}} \right]^{\frac{3}{2}}}{\left[ \left( v_{0,LF}^+ \right)^2 \left( \frac{d^{NB,LF}}{v_{0,LF}^+} \right)^{\frac{2}{k}} + \left( v_{0,HF}^+ \right)^2 \left( \frac{d^{NB,HF}}{v_{0,HF}^+} \right)^{\frac{2}{k}} \right]^{\frac{1}{2}}}, \tag{81}$$

where  $d^{NB,LF}$  and  $d^{NB,HF}$  are obtained by a narrowband formulation (14), associated with the LF and HF components, respectively. The frequency of the positive zero slope crossing for both components is defined by Eq. (52).

*Single-moment method (1990)*. The single-moment method of Lutes and Larsen is an empirical formula that estimates the damage intensity based on  $2/k$ -th spectral moment  $m_{2/k}$  [59,60]:

$$d^{SM} = \frac{2^{k/2}}{2\pi C} \Gamma\left(1 + \frac{k}{2}\right) \left(m_{2/k}\right)^{k/2}. \tag{82}$$

The method was formulated on the basis of a rainflow analysis for a bimodal PSD as an improvement to the narrowband approximation (14). It is clear that for a narrowband process with a central frequency  $\omega_0$ , Eq. (82) converges to the narrowband approximation formula, as  $(m_{2/k})^{k/2} \approx \omega_0 m_0^{k/2}$  and  $v_0^+ = \omega_0/2\pi$ .

*Notes on projection-by-projection (2011)*. Although the single-moment method was elaborated on a purely empirical basis, Benasciutti et al. [55] provided a mathematical interpretation using the Projection-by-Projection (PbP) scheme, in which the fatigue damage due to multiaxial loading is estimated by a suitable non-linear sum of the damage contributions for uncorrelated uniaxial stochastic processes. By decomposing the PSD into  $n$  infinitesimal spectral contributions and summing the corresponding narrowband damage intensities  $d_{NB,i}$  (14) through a quadratic amplitude sum of the PbP method [62], the damage covering all the bands is obtained:

$$d^{PbP} = \left( \sum_{i=1}^n \left( d_{NB,i} \right)^{\frac{2}{k}} \right)^{\frac{k}{2}} \tag{83}$$

which turns out to be the discrete form of the single-moment method (82):

$$d^{PbP} = \left( \sum_{i=1}^n (d^{NB,i})^{\frac{2}{k}} \right)^{\frac{k}{2}} = \left\{ \sum_{i=1}^n \left[ \frac{\omega_i}{2\pi C} \left( \sqrt{2 S_{xx}(\omega_i)} d\omega \right)^k \Gamma\left(1 + \frac{k}{2}\right) \right]^{\frac{2}{k}} \right\}^{\frac{k}{2}}$$

$$= \frac{2^{\frac{k}{2}}}{2\pi C} \Gamma\left(1 + \frac{k}{2}\right) \left[ \sum_{i=1}^n \omega_i^{\frac{2}{k}} S_{xx}(\omega_i) \Delta\omega \right]^{\frac{k}{2}} = d^{SM}. \tag{84}$$

Han–Ma (2016). Han and Ma [64] researched the fatigue damage in the case of a bimodal random process, where they combined fatigue damage subjected to the LF and HF Gaussian random processes and proposed the method:

$$d^{CB} = \left( (d^{NB,LF})^{\frac{2}{k}} + (d^{NB,HF})^{\frac{2}{k}} \right)^{\frac{k}{2}}, \tag{85}$$

where the quadratic amplitude sum of the PbP method (83) is used (for  $n=2$ ).

Bands method (2015). The bands method was proposed by Braccesi et al. [61] and assumes uncorrelated narrowband random processes, whose variance can be summed according to the laws of the combination of random variables. To combine the fatigue damage of all the bands using a simple sum, the condition of the same frequency  $v_{0,ref}^+$  for all the bands is imposed. In this case, the  $i$ th band damage equivalence has to be respected:

$$m_{0,ref,i} = \left( \frac{v_{0,i}^+}{v_{0,ref}^+} \right)^{2/k} m_{0,i} \tag{86}$$

and the reference zero-order moment of a combination process can be evaluated as:

$$m_{0,ref} = \sum_{i=1}^n m_{0,ref,i}. \tag{87}$$

The damage intensity is estimated by the narrowband approximation formula (14) (with the frequency of positive slope zero crossing  $v_{0,ref}^+$  and the variance  $m_{0,ref}$ ):

$$d^{BM} = v_{0,ref}^+ C^{-1} \left( \sqrt{2 m_{0,ref}} \right)^k \Gamma\left(1 + \frac{k}{2}\right), \tag{88}$$

indicating that the proposed fatigue-combination rule is equivalent to a quadratic amplitude sum of the PbP criterion [62,63].

#### 4. Comparison of spectral methods

In general, the spectral load is not narrowband or of any other shape that some of the methods assume. Therefore, an ideal spectral method should be accurate across various spectra and also applicable for different types of material. The reviewed spectral methods are compared to the time-domain rainfall algorithm using the numerical simulations, with the comparison being based on the 104 different PSD spectra and three different fatigue-strength exponents. In addition, the comparison is supported by the FLife [70] package and is fully reproducible using the package documentation. Basic vibration-fatigue spectral-analysis workflow using the FLife is given by example use code in the Appendix.

##### 4.1. Simulated spectra

Similar to Mršnik et al. [15], the researched 104 spectra are arranged in the following categories: spectral width (SW), background noise (BN), close-mode spectra (CM), multi-mode spectra (MM) and typical automotive spectra (AM). To further investigate the applicability of spectral methods for the fatigue analysis of a bimodal Gaussian process, a bimodal spectra (BM) category is additionally researched.

The researched power spectral densities are formed by the superposition of the ideal rectangular spectra (with the exception of the AM spectra). The Vanmarcke bandwidth parameter  $\epsilon_v$  is used to describe the spectral width of each block; though there is no rigorous criterion to distinguish narrowband and broadband random processes, the cases of  $\epsilon_v < 0.1$  are treated as narrowband in practice [84]. In this study, the width of each block is adjusted such that  $\epsilon_v = 0.05$ . The ranges of the Vanmarcke parameter for each spectra category are given in Table 2. All the power spectral densities are defined in the frequency range 10 Hz to 1000 Hz with an RMS value of 10 MPa. The details of the PSD categories are defined in the following paragraphs.

Spectral width (SW). The proposed category is used to research the effect of the spectral width on the accuracy of the spectral methods. With a central frequency of 450 Hz and  $\epsilon_v = 0.05$ , the initial narrowband random process expands in both directions during each iteration, as depicted in Fig. 4(a). In each iteration the Vanmarcke parameter of the random process is increased by 0.05. The number of researched spectra in this category is nine.

**Table 2**  
Ranges of the Vanmarcke parameter  $\epsilon_v$  for each spectra category.

	SW	BN	CM	MM	AM	BM
$\epsilon_v$	0.05–0.45	0.05–0.45	0.12–0.61	0.44–0.47	0.65–0.71	0.12–0.87

**Table 3**  
Bimodal spectra parameters.

$\gamma$	$m_{0,LF}/m_0$	$f_{LF}$ [Hz]
1.5, 2, 2.5, 3, 4, 7, 10, 15, 30	0.1, 0.2, 0.3, ..., 0.8, 0.9	25

**Background noise (BN).** The background-noise category is used to research the effect of the background noise on the accuracy of the spectral methods. The initial process is considered narrowband with a central frequency of 450 Hz and a Vanmarcke parameter of  $\epsilon_v=0.05$ . In each iteration the amplitude of the background noise in the frequency range 10 Hz to 900 Hz is increased, such that the Vanmarcke parameter of the random process increases by 0.05, as depicted in Fig. 4(b). The number of researched spectra in this category is nine.

**Close-mode spectra (CM).** The bimodal random process represents one of the basic forms of an engineering structural dynamic response, so the close-modes spectra category was used to determine the effect of the close modes on the fatigue-life estimate’s accuracy. Two rectangular blocks with a Vanmarcke parameter  $\epsilon_v=0.05$  and central frequencies of 100 and 800 Hz were, at each iteration step, moved closer by 100 Hz, see Fig. 4(c). The number of researched spectra in this category is seven.

**Multimode spectra (MM).** Multimode spectra are prevalent in civil, mechanical and marine engineering. To research the influence of multiple modal frequencies on the fatigue-life spectral estimates, the multimode spectra category is defined. The initial spectrum has three dominant modes and with each subsequent iteration one additional mode is added (up to a maximum of six), as shown in Fig. 4(d). The modes are positioned at the central frequencies of 100, 250, 400, 550, 700 and 850 Hz with the Vanmarcke parameter of each mode being  $\epsilon_v=0.05$ . The number of researched spectra in this category is four.

**Typical automotive spectra (AM).** To test the applicability of spectral methods in real fatigue loads, three realistic spectra that are typical for the automotive industry are used in this category, as shown in Fig. 4(e). The number of researched spectra in this category is three.

**Bimodal spectra (BM).** Since structural components are often subjected to the combined effect of one low-frequency and one high-frequency load, the fatigue analysis of the bimodal Gaussian process has appeared as a topic on its own [51]. Accordingly, a bimodal spectra category is formulated, where a bimodal spectrum is formed by the superposition of two rectangular blocks [51,59], as illustrated in Fig. 4(f). The width of each block is adjusted such that the Vanmarcke parameter is  $\epsilon_v = 0.05$ , ensuring that both components are practically narrowband. These two-block spectra are characterized by the frequency ratio  $\gamma$  and the area ratio  $\beta$  as:

$$\gamma = \frac{f_{HF}}{f_{LF}}, \quad \beta = \frac{\int_{f_{HF,lb}}^{f_{HF,ub}} G_{xx}(f) df}{\int_{f_{LF,lb}}^{f_{LF,ub}} G_{xx}(f) df} = \frac{m_{0,HF}}{m_{0,LF}} = \frac{m_0 - m_{0,LF}}{m_{0,LF}}. \tag{89}$$

Given the frequency ratio  $\gamma$ , the central frequency  $f_{LF}$  and variance  $m_{0,LF}$  of LF mode, the amplitude of both blocks can be determined. In this study, permutations of these parameters are specified in Table 3. Accordingly, the number of researched spectra in this category is 72.

#### 4.2. Fatigue-life estimate relative error

The frequency-domain fatigue-life estimates were compared to the fatigue-life estimate in the time domain using a combination of the rainflow count [3,4,76] and the Palmgren–Miner linear damage-accumulation rule (10). Note that failure occurs when the damage  $D \geq 1$ , but in practice thresholds that are conservatively lower are often used. While  $D = 1$  is adopted in this study, the fatigue life  $T$  is correlated with the damage intensity  $d$  (12) as [1]:

$$T = \frac{1}{d} \tag{90}$$

and the relative error of the fatigue-life estimate  $T_{err}^{xx}$  can be defined as:

$$T_{err}^{xx} = \frac{T^{xx} - T^{RFC}}{T^{RFC}}, \tag{91}$$

where the  $T^{xx}$  designates a fatigue-life estimate, obtained with one of the reviewed methods, whereas the time-domain-based rainflow life  $T^{RFC}$  is assumed to be the exact reference value.

**Applied materials.** The  $S-N$  curve (9) slope  $k$  significantly affects the accuracy of the fatigue-life estimation. Accordingly, this study considers different materials, presented by Petrucci and Zuccarello [66], specified in Table 4.

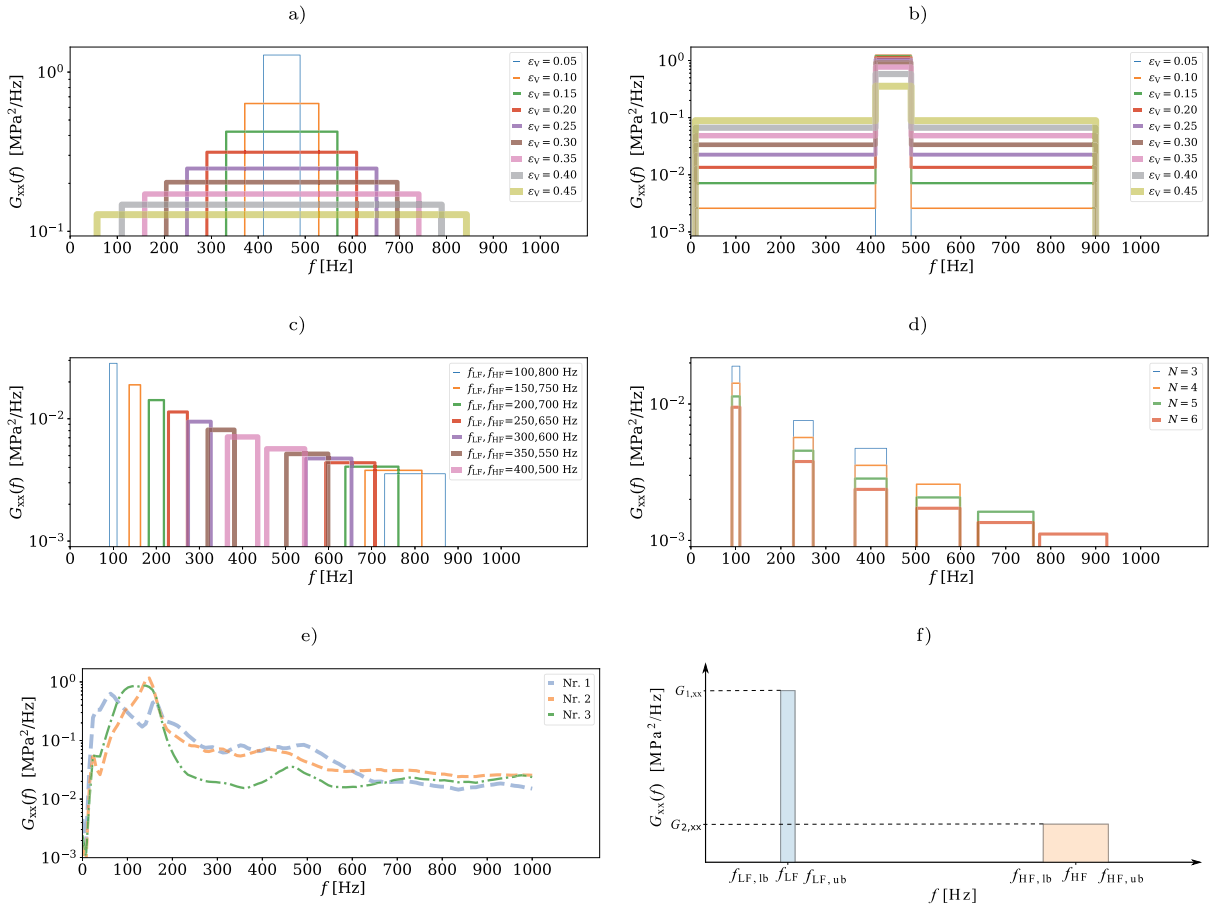


Fig. 4. Researched spectra: (a) spectral width (SW); (b) background noise (BN); (c) close mode spectra (CM); (d) multimode spectra (MM); (e) automotive spectra (AM); (f) bimodal spectra (BM).

Table 4  
S-N curve parameters [66] used in spectral methods comparison.

	C (MPa <sup>k</sup> )	k
Steel	$1.934 \times 10^{12}$	3.324
Aluminium	$6.853 \times 10^{19}$	7.300
Spring steel	$1.413 \times 10^{37}$	11.760

Reference criteria - time-domain analysis. The tree-point rainflow counting (RFC) algorithm [4] as implemented in [85] is used to extract the cycle ranges and the corresponding mean values from the time-domain representation of a random process.

An established procedure to obtain a time series from the PSD involves the discretization of the spectrum into  $N$  components, each of equal frequency interval  $\Delta\omega$ . Then, the time series may be generated as [86]:

$$x(t) = \sum_{k=1}^N A_k \cos(\omega_k t + \phi_k), \tag{92}$$

where the phase angle  $\phi_k$  is uniformly distributed on the interval  $[0, 2\pi)$  and the amplitude  $A_k$  follows a Rayleigh distribution (93) with parameter  $\sigma_{x,k}$  obtained from one-sided spectrum  $W_{xx}(\omega)$ :

$$p_{A_k}(a) = \frac{a}{\sigma_{x,k}^2} e^{-\frac{a^2}{2\sigma_{x,k}^2}}, \quad \sigma_{x,k} = \sqrt{\Delta\omega W_{xx}(\omega_k)}. \tag{93}$$

The sampling frequency  $f_s$  has a fundamental role in the IDFT; for all the frequency components in the PSD to be manifested in the associated time series, the sampling frequency is set according to the Nyquist theorem,  $f_s \geq 2 f_{max}$  [87]. Dirlik [44] pointed out that there should be more than five data points between successive peaks and valleys to produce an adequate stress time-history. Since

**Table 5**  
Percentage of spectral estimates within different margins of relative error for steel,  $k=3.324$  (green), aluminium,  $k=7.3$  (blue) and spring steel,  $k=11.76$  (red).

Spectral method	Relative error											
	< 5%			< 10%			< 20%			< 50%		
	% of spectra			% of spectra			% of spectra			% of spectra		
Narrowband	26	12	4	50	23	14	74	79	48	100	100	100
Wirsching-Light	21	0	0	57	3	3	100	4	3	100	100	56
Ortiz-Chen	98	37	30	100	68	51	100	100	90	100	100	100
$\alpha_{0.75}$	77	43	25	100	74	51	100	97	97	100	100	100
Tovo-Benasciutti 1	31	12	7	55	26	17	80	88	55	100	100	97
Tovo-Benasciutti 2	43	16	17	95	37	30	100	55	53	100	100	91
Dirlik	46	39	28	100	59	64	100	94	89	100	100	100
Zhao-Baker	94	51	45	94	83	58	97	97	88	100	100	100
Park	77	30	16	100	66	58	100	87	81	100	100	100
Jung-Park	84	49	25	100	61	56	100	100	88	100	100	100
Jiao-Moan	6	3	6	11	6	9	41	16	11	93	93	50
Sakai-Okamura	0	0	0	0	0	0	0	0	0	47	0	0
Fu-Cebon	0	0	0	0	0	0	0	0	0	75	31	29
Modified Fu-Cebon	11	3	6	24	6	9	67	21	11	100	93	59
Low (2010) <sup>a</sup>	28	25	3	68	39	3	93	46	26	100	58	29
Low (2014)	25	31	45	84	57	57	100	95	90	100	100	100
Lotsberg	0	0	0	0	0	0	0	0	0	29	0	0
Huang-Moan	55	63	52	94	87	71	100	97	97	100	100	100
Gao-Moan	16	0	0	19	0	0	58	0	0	100	3	0
Single Moment	59	32	19	80	69	60	93	80	77	100	100	100
Bands Method	62	30	17	80	74	55	93	80	77	100	100	100

<sup>a</sup>For Low (2010) method  $k=3$ ,  $k=7$  and  $k=12$  is used for steel, aluminium and spring steel, respectively.

in this research the spectra are defined in the frequency interval 10 Hz to 1000 Hz, the sampling frequency is set to  $f_s = 10 f_{max} = 10$  kHz.

Because the simulated stress time-history is a random process, the RFC fatigue damage is a random variable with the mean value given by Eq. (10). To reduce the uncertainty of the RFC damage, 20 time-histories of one hour are simulated for each spectrum and the average damage is then taken as the reference fatigue damage. The relative error of the RFC damage (averaged over 20 time-histories) for a signal fragment relative to the complete (1 h) time-history fell below 2% at around 2 s of the time-history for steel, at around 150 s for aluminium and at around 2600 s for spring steel. The number of cycles (and half-cycles) counted ranged from  $5 \times 10^6$  to  $4.7 \times 10^7$ , which ensured convergence of the RFC fatigue-life estimate. It should be noted that, from a physical point of view, such a high number of cycles is outside the high cycle fatigue region, where the S-N model is applied.

Once the rainflow matrix is extracted, the cycle mean values are discarded since the discussed spectral methods do not directly address their affect on the fatigue life. Moreover, it has been shown that the rainflow cycle mean stress has a t-location distribution with zero mean [88]. In terms of the fatigue strength a tensile normal mean stress is detrimental and a compressive normal mean stress is beneficial [73]; the effect of the rainflow mean stress can be ignored in the frequency-domain fatigue-life estimation, and only the stress cycle amplitude is considered.

### 4.3. Results

The spectral method comparison results for steel (green), aluminium (blue) and spring steel (red) are detailed in Table 5, where the percentages of estimates for each method that are inside a certain margin of relative error (91) are given, considering a total of 32 spectra (SW, BN, CM, MM and AM spectra category). The reasoning for such a comparison is the fact that the compared methods can be applied to an arbitrary spectra and the user is interested in the method that performs best. For instance, when steel is used the narrowband formulation's relative error is less than 0.1 for 50% of the analyzed spectra, according to Table 5.

Even though some spectral methods are formulated for specific applications, e.g., the bimodal spectral methods are meant to be used for a random stress response that constitutes of two modal peaks, they are compared with methods for general broadband processes. The generalization of the bimodal and trimodal spectral methods to broadband processes is accomplished by splitting the power spectral density into two or three parts, respectively. The criteria for this procedure is arbitrary, however, in this review the splitting is made according to equal variance criteria, with each part then being treated as one of the modes [48].

From Table 5 is clear that the  $S - N$  curve's slope  $k$  affects the accuracy of the spectral methods: with the increase of the fatigue-strength exponent, the fatigue-life estimates become generally less accurate. Because they exhibited the best performance, the Ortiz-Chen (OC),  $\alpha_{0.75}$ , Tovo-Benasciutti 2 (TB2), Dirlik (DK), Zhao-Baker (ZB), Park (PK), Jun-Park (JP) and Huang-Moan (HM) methods were selected for a detailed analysis in the Discussion. Figs. 5–7 show the relative error of the selected estimates for each spectrum in examined spectra categories for steel (OC,  $\alpha_{0.75}$ , TB2, DK, ZB, PK and JP), aluminium (OC,  $\alpha_{0.75}$ , DK, ZB, PK, JP and HM) and spring steel (OC,  $\alpha_{0.75}$ , DK, ZB, PK, JP and HM), respectively. In the figures the Vanmarcke bandwidth parameter (6) is plotted as a secondary  $y$ -axis.

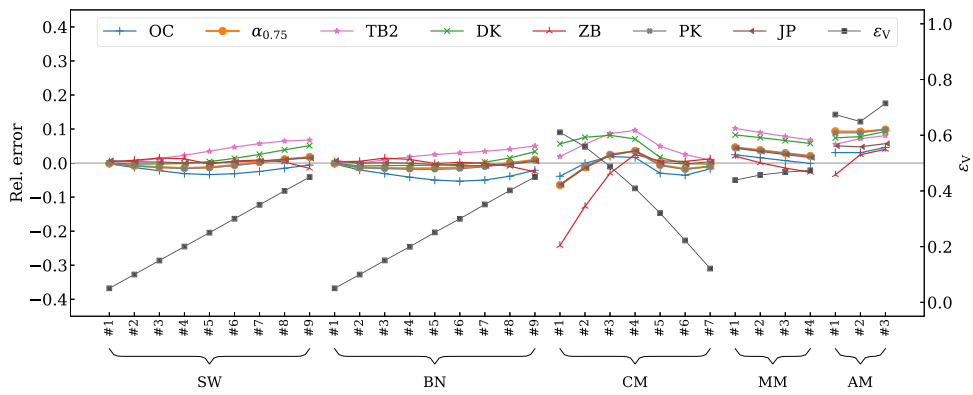


Fig. 5. Comparison of relative errors for steel,  $k = 3.324$ .

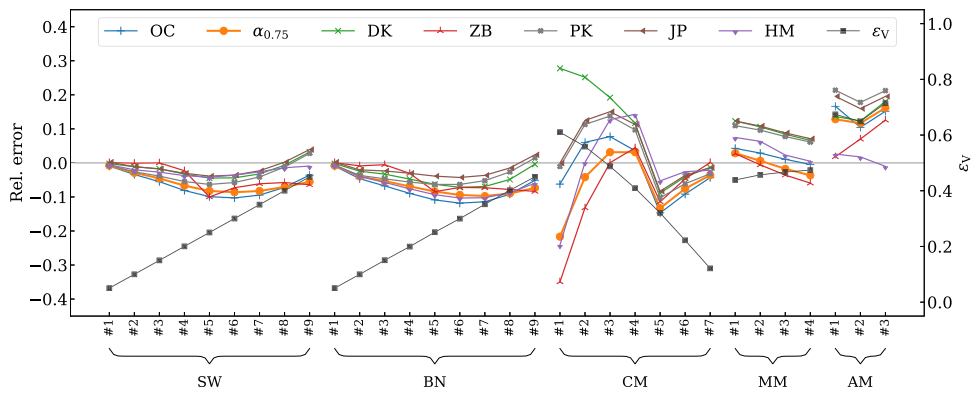


Fig. 6. Comparison of relative errors for aluminium,  $k = 7.3$ .

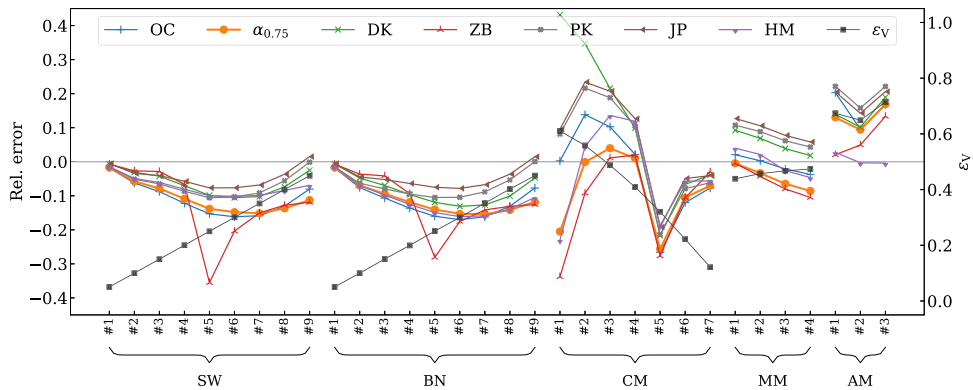


Fig. 7. Comparison of relative errors for spring steel,  $k = 11.76$ .

As the fatigue analysis of the bimodal Gaussian process appeared as a topic on its own [51], a comparison of the bimodal spectral method was conducted on a bimodal spectra category (BM) to further investigate its applicability. Table 6 details the percentages of estimates for each bimodal method that are inside a certain margin of relative error (91). The comparison results for steel (green), aluminium (blue) and spring steel (red) are obtained, considering a total of 72 bimodal spectra (see Table 3).

Because they exhibited the best performance, the Jiao-Moan (JM), Fu-Cebon (FC), modified Fu-Cebon (MFC), Low’s bimodal (2010), Low (2014) and Huang-Moan (HM) methods were selected for a detailed analysis in the Discussion. Figs. 8–10 show the relative errors of the selected estimates for each spectrum in the examined spectra categories for steel (JM, FC, MFC, Low’s bimodal (2010) and Low (2014)), aluminium (JM, FC, MFC, Low (2014) and HM) and spring steel (JM, FC, MFC and HM), respectively.

**Table 6**  
Percentage of spectral estimates within different margins of relative error for  $k=3.324$  (green),  $k=7.3$  (blue) and  $k=11.76$  (red), bimodal spectra.

Spectral method	Relative error											
	5%			10%			20%			50%		
	% of spectra			% of spectra			% of spectra			% of spectra		
Jiao-Moan	65	8	8	74	22	12	85	47	28	100	96	72
Sakai-Okamura	6	0	0	11	1	0	26	4	1	61	18	4
Fu-Cebon	0	6	1	18	14	8	42	39	28	100	76	60
Modified Fu-Cebon	42	8	8	69	18	14	89	40	26	100	96	69
Low (2010) <sup>a</sup>	100	67	28	100	72	51	100	78	57	100	82	60
Low (2014)	89	78	15	100	92	62	100	99	79	100	100	90
Lotsberg	0	0	0	1	0	0	11	0	0	74	6	0
Huang-Moan	32	36	26	49	43	39	76	58	53	93	92	89

<sup>a</sup>For Low (2010) method  $k=3$ ,  $k=7$  and  $k=12$  is used for steel, aluminium and spring steel, respectively.

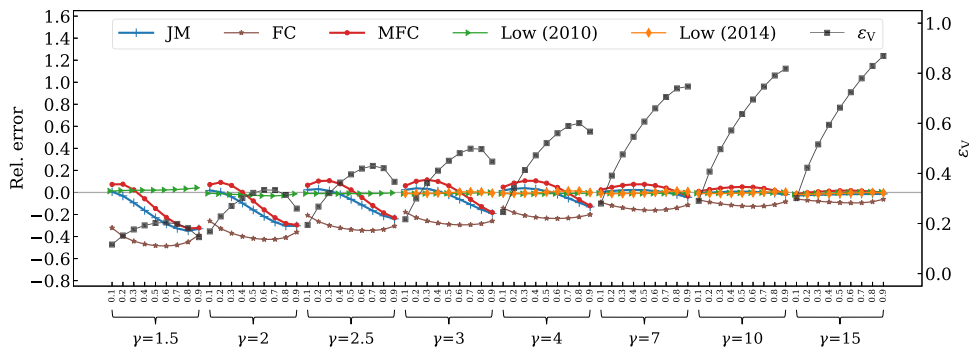


Fig. 8. Comparison of relative errors for steel,  $k = 3.324$ , bimodal spectra.

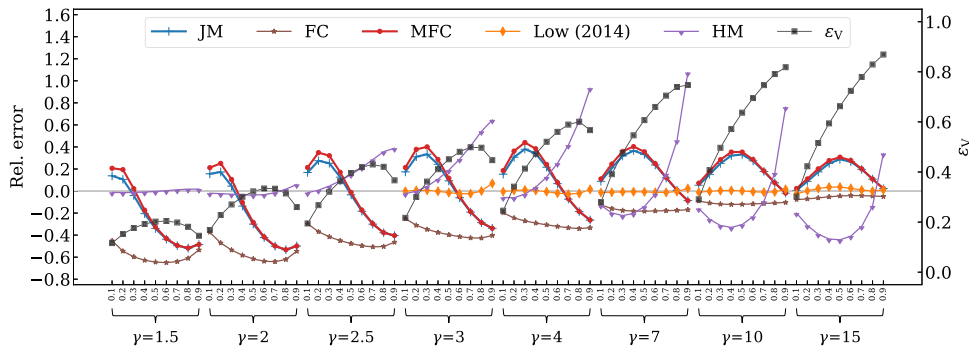


Fig. 9. Comparison of relative errors for aluminium,  $k = 7.3$ , bimodal spectra.

**5. Discussion**

An ideal damage-estimation method for use in a design process should be consistent across different spectra and different slopes of the  $S-N$  curve. To guarantee a safe design it is preferable for the spectral method to be conservative when not accurate; however, this could possibly result in economic losses. What follows is a brief discussion on the accuracy of the selected methods for each spectral category.

For each material the best-performing spectral methods were selected for a detailed analysis based on Tables 5 and 6. Note that it is nonconservative to underestimate the damage intensity, as the fatigue life will be overestimated. The relative error  $T_{err}^{xx}$  (91) of the selected methods with respect to the RFC scheme is shown in Figs. 5–10, with the Vanmarcke bandwidth parameter (6) being plotted on the secondary  $y$ -axis.

*Spectral width.* For steel, the best performing spectral methods exhibit a relative error less than 7%. OC is the most conservative method, whereas TB2 is strictly nonconservative. With an increase of the exponent  $k$ , the fatigue-life estimates tend to become more conservative. The relative error is increased, although it is still below 10% and 17% (with one exception of a ZB estimate) for

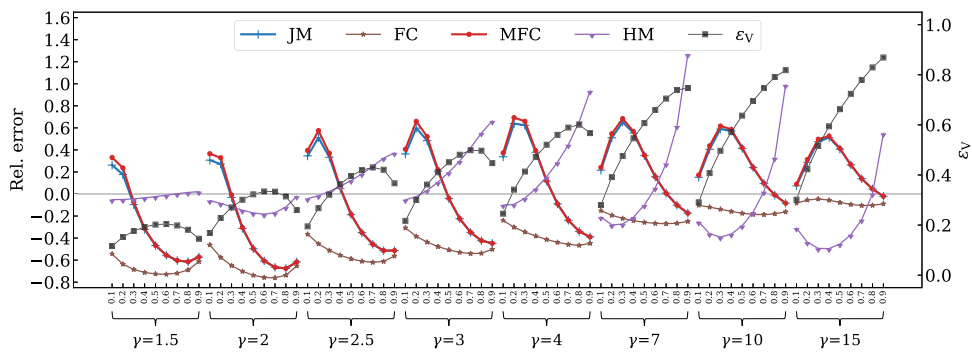


Fig. 10. Comparison of relative errors for spring steel,  $k = 11.76$ , bimodal spectra.

aluminium and spring steel, respectively. The JP method is the most accurate of the selected methods, with a relative error below 7% for all the materials.

**Background noise.** In the case of the background noise category, the fatigue-life estimates have a similar trend as for the spectral width category. The OC and TB2 methods are again the most and the least conservative, respectively. The relative error is below 12% for the aluminium and below 18% for the spring steel (with one exception of a ZB estimate), where the majority of the estimates are conservative. The method that performs best is the JP method, regardless of the value of  $k$ .

**Close mode spectra.** With the exception of the ZB method, all the best-performing methods have relative error below 10% in the case of steel. When the modes are farther apart, the ZB method gives a very conservative estimate, with a relative error up to 25%. For aluminium and steel, the relative error is below 25%, except for the DK and ZB methods with relative errors up to 40%. A significant dependency of the estimates on the Vanmarcke parameter can be observed for all the methods.

**Multimode spectra.** For steel the relative error is below 10% for all the best-performing methods. Except for the ZB method, the fatigue-life estimates are nonconservative. With an increase of the exponent  $k$ , the relative error is under 15% for both aluminium and spring steel. For all the materials, the ZB is the most conservative method, with a relative error below 10%.

**Typical automotive spectra.** For steel the relative error is below 10% for all the in-detail-discussed methods. With an increase of the parameter  $k$  the spectral methods become nonconservative with a relative error below 25% for aluminium and spring steel. The HM method exhibits great accuracy, with the relative error below 5% for all the materials.

**Bimodal spectra.** Low's bimodal (2010) method is the most comprehensive; however, because the damage intensity due to large stress cycles is approximated through the McLaurin series, sufficient engineering precision is up to  $k=6$  [52] and the method was applied only for steel. The relative error for Low's bimodal method is below 5%, when the central frequency ratio is  $\gamma \leq 2$ . For larger  $\gamma$  the relative error is below 2%, with the estimates being conservative.

The Low (2014) method [53] also has good accuracy, with a relative error below 2% for steel and 5% for aluminium. As the method is devised for  $\gamma \geq 3$  and  $3 \leq k \leq 8$ , it was not applied to spring steel.

The FC method is always conservative, within the relative error below 50%, 65% and 75% for steel, aluminium and spring steel, respectively. With an increase of the central frequency ratio  $\gamma$ , the relative error becomes smaller (e.g., below 10% for  $\gamma=15$ ).

For steel the relative error of the JM and MFC methods is below 35% when  $\gamma=1.5$  and is reduced with a larger central frequency ratio (e.g., for  $\gamma=15$  the relative error is below 5%). For aluminium and spring steel the relative error is increased. Both methods are very dependent on the Vanmarcke bandwidth parameter.

The HM method gives good predictions only in a small bandwidth range, e.g., for all the researched materials the relative error is below 5% when  $\gamma=1.5$ , whereas the error is up to 20% when  $\gamma=2$ .

## 6. Conclusion

This research reviews the spectral domain fatigue analysis of Gaussian broadband random process. The well-established and also recent spectral methods for fatigue-life estimation are presented in the same theoretical framework. Analogies and differences among more than 20 spectral methods are discussed. Based on the 104 defined spectra, the corresponding time-histories are numerically simulated and the rainflow algorithm is then applied to obtain the reference fatigue life, where three different materials are considered: steel, aluminium and spring steel. The side-by-side comparison of the spectral method is conducted in the sense that they perform well, regardless of the response spectrum and material being analyzed.

A group of best-performing methods is selected for each material, which can be applied to a general broadband spectra. If a total of 32 loads (all spectra apart those from bimodal spectra category) are evaluated, for small values of the  $S-N$  curve slope ( $k=3.324$ ) the majority of the best performing methods (Ortiz-Chen,  $\alpha_{0.75}$ , Tovo-Benasciutti 2, Dirlik, Park, Jun-Park) give fatigue-life estimates within an acceptable engineering accuracy. The exception to this is the Zhao-Baker method, which is very conservative

in the case of well separated modes. As the fatigue-strength exponent increases ( $k=7.3$ ), the choice of acceptable spectral methods is reduced to the Ortiz Chen,  $\alpha_{0.75}$ , Park, Jun-Park and Huang-Moan methods with the relative error being below 25%. Even if the Huang-Moan method is devised for bimodal random processes, it exhibits remarkable accuracy for broadband processes by splitting the PSD according to the equal variance criterion. For extreme values of  $k$  ( $k=11.76$ ) the fatigue-life error is further increased and the acceptable spectral methods are again Ortiz-Chen,  $\alpha_{0.75}$ , Park, Jun-Park and Huang-Moan with relative errors up to 25%.

A detailed analysis of bimodal spectral methods is performed on the basis of 72 bimodal spectra, where the central frequency ratio  $\gamma$  and variance ratio  $\beta$  were permuted. For small values of the fatigue-strength exponent ( $k=3.324$ ) the Low's bimodal method exhibited best accuracy with a relative error below 5%, even for small values of  $\gamma$ . Another method that performs well is the Low 2014 method; however, Low 2014 is limited to  $\gamma \geq 3$ . The Jiao-Moan and modified Fu-Cebon methods become sufficiently accurate with larger frequency ratio, e.g., for  $\gamma=10$  the relative error falls below 5%. For higher slope of the  $S-N$  curve ( $k=7.3$ ) only the Low 2014 method has a relative error below 5%. The accuracy of the Fu-Cebon method is improved as the frequency ratio increases; for  $\gamma=15$  the relative error is below 10% for all the researched materials. Conversely, for the small bandwidth range the Huang-Moan method is considered accurate, e.g., for  $\gamma=1.5$  the relative error is below 5%, regardless of the analysed material.

This research highlights the applicability of spectral methods for use in vibration fatigue. From the comparison of more than 20 spectral methods, other methods besides well-established ones, such as the Dirlik and Tovo-Benasciutti methods, should be considered when the fatigue load is broadband: the Ortiz-Chen,  $\alpha_{0.75}$ , Park, Jun-Park and Huang-Moan methods. Furthermore, as the fatigue analysis of bimodal random processes has become well established, the applicability of bimodal methods is inspected. Among the reviewed spectral methods, Low's bimodal and the Low 2014 method show exceptional accuracy that can be attained using the bimodal formulation.

### Declaration of competing interest

The authors declare that they have no known competing financial interests or personal relationships that could have appeared to influence the work reported in this paper.

### Data availability

The source-code including all supported measurement data is available and published at <https://github.com/ladisk/FLife>.

### Acknowledgments

The authors acknowledge the partial financial support from the Slovenian Research Agency (research core funding no. P2-0263).

### Appendix. FLife code example

The following code shows basic vibration-fatigue spectral-analysis workflow using the FLife [70] open-source Python package.

```
import FLife
import numpy as np

dt = 1e-4
x = np.random.normal(scale=100, size=10000)

C = 1.8e+22 # S-N curve intercept [MPa**k]
k = 7.3 # S-N curve inverse slope [/]

# Spectral data
sd = FLife.SpectralData(input=(x, dt))

# Rainflow reference fatigue life
# (do not be confused here, spectral data object also holds the time domain data)
rf = FLife.Rainflow(sd)

# Spectral methods
dirlik = FLife.Dirlik(sd)
tb = FLife.TovoBenasciutti(sd)
print(f'          Rainflow: {rf.get_life(C = C, k=k):4.0f} s')
print(f'          Dirlik: {dirlik.get_life(C = C, k=k):4.0f} s')
print(f'Tovo Benasciutti 2: {tb.get_life(C = C, k=k, method="method 2"):4.0f} s')
```

## References

- [1] J. Slavič, M. Mršnik, M. Česnik, J. Javh, M. Boltežar, *Vibration Fatigue by Spectral Methods*, Elsevier, 2020.
- [2] D.E. Newland, *An Introduction to Random Vibrations, Spectral & Wavelet Analysis*, Dover Publications, 2005.
- [3] M. Matsuishi, T. Endo, Fatigue of metals subjected to varying stress, *Japan Soc. Mech. Eng. Fukuoka, Japan* 68 (2) (1968) 37–40.
- [4] ASTM E1049, *Standard Practice for Cycle Counting in Fatigue Analysis*, Standard, Philadelphia, PA, 1985.
- [5] N. Bishop, F. Sherratt, A theoretical solution for the estimation of “rainflow” ranges from power spectral density data, *Fatigue Fract. Eng. Mater. Struct.* 13 (4) (1990) 311–326.
- [6] A. Palmgren, Die Lebensdauer von Kugellagern, *Zeitschrift Des Vereines Deutscher Ingenieure* 68 (14) (1924) 339–341.
- [7] M.A. Miner, Cumulative damage in fatigue, *J. Appl. Mech.* 67 (1945) A159–A164.
- [8] C. Stromeyer, The determination of fatigue limits under alternating stress conditions, *Proc. R. Soc. Lond. Ser. A* 90 (620) (1914) 411–425.
- [9] J. Spindel, E. Haibach, Some Considerations in the Statistical Determination of the Shape of S-N Curves, *ASTM Special Technical Publications*, 1981, pp. 89–113.
- [10] F. Stüssi, *Die Theorie Des Dauerfestigkeit Und Die Versuche Von August Wöhler*, Verlag VSB, 1955.
- [11] J. Kohout, S. Vechet, A new function for fatigue curves characterization and its multiple merits, *Int. J. Fatigue* 23 (2) (2001) 175–183.
- [12] M. Muñiz-Calvente, A. Álvarez-Vázquez, F. Pelayo, M. Aenlle, N. García-Fernández, M. Lamela-Rey, A comparative review of time- and frequency-domain methods for fatigue damage assessment, *Int. J. Fatigue* 163 (2022) 107069.
- [13] I. Rychlik, Fatigue and stochastic loads, *Scand. J. Stat.* (1996) 387–404.
- [14] R. Tovo, Cycle distribution and fatigue damage under broadband random loading, *Int. J. Fatigue* 24 (11) (2002) 1137–1147.
- [15] M. Mršnik, J. Slavič, M. Boltežar, Frequency-domain methods for a vibration-fatigue-life estimation - Application to real data, *Int. J. Fatigue* 47 (2013) 8–17.
- [16] M. Mršnik, J. Slavič, M. Boltežar, Vibration fatigue using modal decomposition, *Mech. Syst. Signal Process.* 98 (2018) 548–556.
- [17] Y. Zhou, J. Tao, Theoretical and numerical investigation of stress mode shapes in multi-axial random fatigue, *Mech. Syst. Signal Process.* 127 (2019) 499–512.
- [18] W. Lei, Y. Jiang, X. Zeng, Z. Fan, Research on the transmission law of kurtosis of SDOF system under nonstationary and non-Gaussian random excitations, *Mech. Syst. Signal Process.* 165 (2022) 108292.
- [19] R. Zheng, G. Chen, H. Chen, Power spectrum and kurtosis separation method for multi-shaker non-Gaussian random vibration control, *Mech. Syst. Signal Process.* 162 (2022) 108015.
- [20] G. D’Elia, E. Mucchi, G. Dalpiaz, A novel methodology for dynamic response maximisation in multi-axis accelerated random fatigue testing, *Mech. Syst. Signal Process.* 181 (2022) 109491.
- [21] S. Cui, R. Geng, C. Wang, C. Cheng, Study of the amplitude modulation method for kurtosis control purposes, *Mech. Syst. Signal Process.* 179 (2022) 109399.
- [22] F. Li, H. Wu, P. Wu, Vibration fatigue dynamic stress simulation under non-stationary state, *Mech. Syst. Signal Process.* 146 (2021) 107006.
- [23] A. Trapp, P. Wolfsteiner, Estimating higher-order spectra via filtering-averaging, *Mech. Syst. Signal Process.* 150 (2021) 107256.
- [24] A. Nieslony, E. Macha, *Spectral Method in Multiaxial Random Fatigue*, Vol. 33, Springer Science & Business Media, 2007.
- [25] X. Pei, S. Krishnan Ravi, P. Dong, X. Li, X. Zhou, A multi-axial vibration fatigue evaluation procedure for welded structures in frequency domain, *Mech. Syst. Signal Process.* 167 (2022) 108516.
- [26] A. Nieslony, Determination of fragments of multiaxial service loading strongly influencing the fatigue of machine components, *Mech. Syst. Signal Process.* 23 (8) (2009) 2712–2721.
- [27] D. Benasciutti, R. Tovo, Fatigue life assessment in non-Gaussian random loadings, *Int. J. Fatigue* 28 (7) (2006) 733–746.
- [28] F. Cianetti, M. Palmieri, C. Braccisi, G. Morettini, Correction formula approach to evaluate fatigue damage induced by non-Gaussian stress state, *J. Sound Vib.* 8 (2018) 390–398.
- [29] P. Wolfsteiner, A. Trapp, Fatigue life due to non-Gaussian excitation – An analysis of the fatigue damage spectrum using higher order spectra, *Int. J. Fatigue* 127 (2019) 203–216.
- [30] P. Wolfsteiner, Fatigue assessment of non-stationary random vibrations by using decomposition in Gaussian portions, *Int. J. Mech. Sci.* 127 (2016).
- [31] A. Trapp, P. Wolfsteiner, Frequency-domain characterization of varying random vibration loading by a non-stationarity matrix, *Int. J. Fatigue* 146 (2021) 106115.
- [32] A. Trapp, P. Wolfsteiner, Fatigue assessment of non-stationary random loading in the frequency domain by a quasi-stationary Gaussian approximation, *Int. J. Fatigue* 148 (2021) 106214.
- [33] F. Kihm, A. Halfpenny, N.S. Ferguson, Fatigue life from Sine-on-random excitations, *Procedia Eng.* 101 (2015) 235–242.
- [34] A. Angeli, B. Cornelis, M. Troncosi, Synthesis of Sine-on-random vibration profiles for accelerated life tests based on fatigue damage spectrum equivalence, *Mech. Syst. Signal Process.* 103 (2018) 340–351.
- [35] G. Zucca, M. Palmieri, F. Cianetti, On the statistical distribution of the maxima of sine on random process, *Mech. Syst. Signal Process.* 158 (2021) 107726.
- [36] J.S. Bendat, A.G. Piersol, *Random Data: Analysis and Measurement Procedures*, Wiley India, 2013.
- [37] J.S. Bendat, *Probability Functions for Random Response: Prediction of Peaks, Fatigue Damage and Catastrophic Failures*, Tech. Rep., NASA, 1964.
- [38] D. Benasciutti, R. Tovo, On fatigue damage assessment in bimodal random processes, *Int. J. Fatigue* 29 (2) (2007) 232–244.
- [39] I. Rychlik, On the ‘narrow-band’ approximation for expected fatigue damage, *Probab. Eng. Mech.* 8 (1) (1993) 1–4.
- [40] P.H. Wirsching, M.C. Light, Fatigue under wide band random stresses, *J. Struct. Div.* 106 (7) (1980) 1593–1607.
- [41] K. Ortiz, N. Chen, Fatigue damage prediction for stationary wideband processes, in: *Fifth International Conference on Applications of Statistics and Probability in Soil and Structural Engineering*, 1987.
- [42] D. Benasciutti, R. Tovo, Rainflow Cycle Distribution and Fatigue Damage in Gaussian Random Loadings, *Tech. Rep.*, University of Ferrara, Department of Engineering, 2004.
- [43] D. Benasciutti, R. Tovo, Spectral methods for lifetime prediction under wide-band stationary random processes, *Int. J. Fatigue* 24 (11) (2002) 1137–1147.
- [44] T. Dirlik, *Application of Computers in Fatigue Analysis* (Ph.D. thesis), University of Warwick, 1985.
- [45] W. Zhao, M.J. Baker, On the probability density function of rainflow stress range for stationary Gaussian processes, *Int. J. Fatigue* 14 (2) (1992) 121–135.
- [46] J.-B. Park, J. Choung, K.-S. Kim, A new fatigue prediction model for marine structures subject to wide band stress process, *Ocean Eng.* 76 (2014) 144–151.
- [47] S.-H. Jun, J.-B. Park, Development of a novel fatigue damage model for Gaussian wide band stress responses using numerical approximation methods, *Int. J. Nav. Archit. Ocean Eng.* 12 (2020) 755–767.
- [48] G. Jiao, T. Moan, Probabilistic analysis of fatigue due to Gaussian load processes, *Probab. Eng. Mech.* 5 (2) (1990) 76–83.
- [49] S. Sakai, H. Okamura, On the distribution of rainflow range for Gaussian random processes with bimodal PSD, *JSMSE Int. J. Ser. A* 38 (4) (1995) 440–445.
- [50] T. Fu, D. Cebon, Predicting fatigue lives for bi-modal stress spectral densities, *Int. J. Fatigue* 22 (1) (2000) 11–21.
- [51] D. Benasciutti, R. Tovo, Comparison of spectral methods for fatigue damage assessment in bimodal random processes, in: *9th International Conference on Structural Safety & Reliability, ICOSSAR*, 2005.
- [52] Y.M. Low, A method for accurate estimation of the fatigue damage induced by bimodal processes, *Probab. Eng. Mech.* 25 (1) (2010) 75–85.
- [53] Y.M. Low, A simple surrogate model for the rainflow fatigue damage arising from processes with bimodal spectra, *Mar. Struct.* 38 (2014) 72–88.

- [54] Z. Gao, T. Moan, Frequency-domain fatigue analysis of wide-band stationary Gaussian processes using a trimodal spectral formulation, *Int. J. Fatigue* 30 (10-11) (2008) 1944–1955.
- [55] D. Benasciutti, A. Cristofori, R. Tovo, Analogies between spectral methods and multiaxial criteria in fatigue damage evaluation, *Probab. Eng. Mech.* 31 (2013) 39–45.
- [56] D. Benasciutti, F. Sherratt, A. Cristofori, Recent developments in frequency domain multi-axial fatigue analysis, *Int. J. Fatigue* 91 (2016) 397–413.
- [57] I. Lotsberg, Background for revision of DNV-RP-C203 fatigue analysis of offshore steel structure, in: 24th International Conference on Offshore Mechanics and Arctic Engineering, ASME, Halkidiki, Greece, 2005, Paper No. OMAE2005-67549.
- [58] W. Huang, T. Moan, Fatigue under combined high and low frequency loads, in: 25th International Conference on Offshore Mechanics and Arctic Engineering, ASME, Hamburg, Germany, 2006, Paper No. OMAE2006-92247.
- [59] L.D. Lutes, C.E. Larsen, Improved spectral method for variable amplitude fatigue prediction, *J. Struct. Eng. ASCE* 116 (4) (1990) 1149–1164.
- [60] C.E. Larsen, L.D. Lutes, Predicting the fatigue life of offshore structures by the single-moment spectral method, *Probab. Eng. Mech.* 6 (2) (1991) 96–108.
- [61] C. Braccetti, F. Cianetti, L. Tomassini, Random fatigue. A new frequency domain criterion for the damage evaluation of mechanical components, *Int. J. Fatigue* 70 (2015) 417–427.
- [62] A. Cristofori, D. Benasciutti, R. Tovo, A stress invariant based spectral method to estimate fatigue life under multiaxial random loading, *Int. J. Fatigue* 33 (7) (2011) 887–899.
- [63] D. Benasciutti, C. Braccetti, F. Cianetti, A. Cristofori, R. Tovo, Fatigue damage assessment in wide-band uniaxial random loadings by PSD decomposition: Outcomes from recent research, *Int. J. Fatigue* 91 (1) (2016) 248–250.
- [64] C. Han, Y. Ma, X. Qu, M. Yang, P. Qin, A practical method for combination of fatigue damage subjected to low-frequency and high-frequency Gaussian random processes, *Appl. Ocean Res.* 60 (2016) 47–60.
- [65] D. Benasciutti, R. Tovo, Comparison of spectral methods for fatigue analysis of broad-band Gaussian random processes, *Probab. Eng. Mech.* 21 (4) (2006) 287–299.
- [66] G. Petrucci, B. Zuccarello, Fatigue life prediction under wide band random loading, *Fatigue Fract. Eng. Mater. Struct.* 27 (12) (2004) 1183–1195.
- [67] C.E. Larsen, T. Irvine, A review of spectral methods for variable amplitude fatigue prediction and new results, *Procedia Eng.* 101 (2015) 243–250.
- [68] A. Wöhler, Versuche über die Festigkeit der Eisenbahnwagen Achsen, *Zeitschrift für Bauwesen* 10 (1860) 160–161.
- [69] J. Quigley, Y.-L. Lee, L. Wang, Review and assessment of frequency-based fatigue damage models, *SAE Int. J. Mater. Manuf.* 9 (2016) 565–577.
- [70] A. Zorman, M. Mršnik, J. Slavič, *FLife*, <http://dx.doi.org/10.5281/zenodo.7417587>. Version: 1.4.1.
- [71] L.D. Lutes, S. Sarkani, *Stochastic Analysis of Structural and Mechanical Vibrations*, Prentice Hall, 1997.
- [72] L.D. Lutes, M. Corazao, S.-I.J. Hu, J. Zimmerman, Stochastic fatigue damage accumulation, *J. Struct. Eng.* 110 (11) (1984) 2585–2601.
- [73] Y.-L. Lee, J. Pan, R. Hathaway, M. Barkey, *Fatigue Testing and Analysis: Theory and Practice*, Butterworth-Heinemann, 2005.
- [74] E.H. Vanmarcke, Properties of spectral moments with applications to random vibration, *J. Eng. Mech. Div.* 98 (2) (1972) 425–446.
- [75] S.O. Rice, Mathematical analysis of random noise, *Bell Syst. Tech. J.* 24 (1) (1945) 46–156.
- [76] C. Amzallag, J.P. Gerey, J.L. Robert, J. Bahuaud, Standardization of the rainflow counting method for fatigue analysis, *Int. J. Fatigue* 6 (4) (1994) 287–293.
- [77] N.E. Dowling, Fatigue failure predictions for complicated stress-strain histories, *J. Mater.* 7 (1) (1972) 71–87.
- [78] J.W. Miles, On structural fatigue under random loading, *J. Aeronaut. Sci.* 21 (11) (1954) 753–762.
- [79] M. Frendahl, I. Rychlik, Rainflow analysis: Markov method, *Int. J. Fatigue* 15 (1993) 265–272.
- [80] H.O. Madsen, S. Krenk, N.C. Lind, *Methods of Structural Safety*, Dover Publications, 2006.
- [81] D. Benasciutti, *Fatigue Analysis of Random Loadings* (Ph.D. thesis), University of Ferrara, 2004.
- [82] G. DNV, *Fatigue Design of Offshore Steel Structures, Recommended Practice DNVGL-RP-C203*, Vol. 20, 2016.
- [83] D.N. Veritas, *Fatigue methodology of offshore ships, Recommended Practice DNV-RP-C206*, 2010.
- [84] G. Shan, Z. Xiang Yuan, An improved spectral discretization method for fatigue damage assessment of bimodal Gaussian processes, *Int. J. Fatigue* 119 (2019) 268–280.
- [85] P. Janiszewski, *rainflow*, Version: 3.1, <https://github.com/iamlikeme/rainflow>.
- [86] M. Giuclea, A.-M. Mitu, O. Solomon, Generation of stationary Gaussian time series compatible with given power spectral density, *Proc. Rom. Acad. Ser. A* 15 (2014) 292–299.
- [87] K. Shin, J.K. Hammond, *Fundamentals of Signal Processing for Sound and Vibration Engineers*, John Wiley & Sons Ltd, 2008.
- [88] Q. Han, J. Li, J. Xu, F. Ye, A. Carpinteri, G. Lacidogna, A new frequency domain method for random fatigue life estimation in a wide-band stationary Gaussian random process, *Fatigue Fract. Eng. Mater. Struct.* 42 (1) (2018) 97–113.